

**BIODEGRADATION RATE OF *Bombyx mori* SILK FIBROIN
THROUGH GAMMA RADIATION FOR
BIOMEDICAL APPLICATIONS**

AMORNTHAP KOJTHUNG

**A THESIS SUBMITTED IN PARTIAL FULFILLMENT
OF THE REQUIREMENTS FOR
THE DEGREE OF MASTER OF ENGINEERING
(BIOMEDICAL ENGINEERING)
FACULTY OF GRADUATE STUDIES
MAHIDOL UNIVERSITY**

2007

COPYRIGHT OF MAHIDOL UNIVERSITY

Thesis
Entitled

**BIODEGRADATION RATE OF *Bombyx mori* SILK FIBROIN
THROUGH GAMMA RADIATION FOR
BIOMEDICAL APPLICATIONS**

.....
Mr. Amornthep Kojthung
Candidate

.....
Assist.Prof. Bovornlak Oonkhanond,
Ph.D. (Chemical Engineering)
Major-Advisor

.....
Prof. Rachanee Udomsangpetch,
Ph.D. (Immunology)
Co-Advisor

.....
Prof. M.R. Jisnuson Svasti,
Ph.D.
Dean
Faculty of Graduate Studies

.....
Assist.Prof. Theeraporn Rubcumintara,
Ph.D. (Materials Engineering & Science)
Chair
Master of Engineering Programme in
Biomedical Engineering
Faculty of Engineering

Thesis
Entitled

**BIODEGRADATION RATE OF *Bombyx mori* SILK FIBROIN
THROUGH GAMMA RADIATION FOR
BIOMEDICAL APPLICATIONS**

was submitted to the Faculty of Graduate Studies, Mahidol University
for the degree of Master of Engineering (Biomedical Engineering)

on
23 May, 2007

.....
Mr. Amornthep Kojthung
Candidate

.....
Assist.Prof. Theeraporn Rubcumintara,
Ph.D. (Materials Engineering & Science)
Chair

.....
Prof. Rachanee Udomsangpetch,
Ph.D. (Immunology)
Member

.....
Assist.Prof. Bovornlak Oonkhanond,
Ph.D. (Chemical Engineering)
Member

.....
Lertyot Treeratanapiboon,
Ph.D. (Medical Technology)
Member

.....
Assist.Prof. Udom Tipayamontri,
Ph.D. (Physiology)
Member

.....
Prof. M.R. Jisnuson Svasti,
Ph.D.
Dean
Faculty of Graduate Studies
Mahidol University

.....
Assist.Prof. Piya Rattanasuwan,
M.Eng.
Dean
Faculty of Engineering
Mahidol University

ACKNOWLEDGEMENT

I would like to express my gratefulness to all who gave me the extensive support and assistance to complete this thesis. First, I would like to thank my thesis advisor, Asst. Prof. Dr. Bovornlak Oonkhanond, for his valuable suggestions and encouragement throughout my work. I am also very grateful to my thesis co-advisor, Prof. Dr. Rachanee Udomsangpetch, for her valuable advice including her great support in my cell culture work. I would like to express my appreciation to all members of the advisory committee, Asst. Prof. Dr. Udom Tipayamontri for his comments, Dr. Lertyot Treeratanapiboon for his kindness and assistance through the time in the tissue culture laboratory, and also Asst. Prof. Dr. Theeraporn Rubcumintara for her comments and advice.

I am especially grateful to Mr. Prateep Meesilpa, the director of the Queen Sirikit Sericulture Regional Office of Northern Part (Phrae Province), for his kindness and support of all silk samples. Moreover, I am sincerely thankful to him again for all knowledge of sericulture and *Bombyx mori* silks, including the silk degumming method which is his patent.

I would like to give my special thanks to Mrs. Boonya Sudatis, a chief of Radiation Entomology Section, Office of Atoms for Peace, for her kindness and support of all facilities while practicing in her laboratory, and for the knowledge of silk film preparation.

I would like to thank Mr. Suriya Patcha at the Office of Atoms for Peace, who gave me knowledge of gamma radiation, and also doing an irradiation part to all of my silk samples.

I also thank all my friends and programme officers at the Biomedical Engineering Programme and at the malaria research laboratory, who are too numerous to name here for their help and everything they have done for me.

Finally, I would like to thank my parents for their love, teaching and financial support that enable me to get to this point in my life. The usefulness of this thesis, I dedicate to my parents and all the teachers who have taught me.

Amornthep Kojthung

BIODEGRADATION RATE OF *Bombyx mori* SILK FIBROIN THROUGH GAMMA RADIATION FOR BIOMEDICAL APPLICATIONS

AMORNTHAP KOJTHUNG 4736139 EGBE/M

M. Eng. (BIOMEDICAL ENGINEERING)

THESIS ADVISORS: BOVORNLAK OONKHANOND, Ph.D. (CHEMICAL ENGINEERING), RACHANEE UDOMSANGPETCH, Ph.D. (IMMUNOLOGY)

ABSTRACT

Silk has been utilized in biomedicine for centuries especially as suture silks. This suture silk is usually produced with silkworm silk, which is the strongest natural protein fiber consisting of two fibroin cores coated with a glue-like protein called sericin. However, the biocompatibility of silks has been a problem for a long period of time possibly due to the residual sericin on silk fibroin. Moreover, some adverse effects were observed in some cases even though the sericin was removed. This problem was investigated and it was found that the slow biodegradation rate of silk fibroin could cause these adverse effects in some patients. Therefore, an attempt to reduce the degradation period of silk fibroin through gamma radiation was then studied.

Thai-native silks, *Bombyx mori* var. *Nangnoi Sisaket-1*, were chosen for this study. Various doses of irradiation were applied to the silk fibroin fibers before in vitro biodegradation testing by protease. The results showed that the degradation rate of silk increased with increasing radiation intensity. This could be determined from a weakness of peptide bonds in fibroin's polypeptides, reduction of crystallinity degree of silk fibroin, loss of fibroin mass, increasing of cleft on the fibers, and releasing of aromatic amino acids including low-molecular weight proteins in degradation products. Although gamma radiation could provide fast-degrading silks, it also affected the cell attachment on silk fibers by reducing the number of attached cells on the fibers when a higher dose of irradiation was applied. Additionally, a preliminary result of an in vitro biocompatibility test showed that there was no activation from human white blood cells to the prepared silk fibroin indicating that it was safe to be used in humans. Thus, this study indicates that Thai silks show promising properties to be developed as biomaterials or for other biomedical applications in the future.

KEY WORDS: SILK FIBROIN/ BIODEGRADATION/ GAMMA RADIATION

67 pp.

การศึกษาการสลายตัวของเส้นไหมที่ผ่านการฉายรังสีด้วยรังสีแกมมาเพื่อนำไปใช้ประโยชน์ทาง
ชีวการแพทย์ (BIODEGRADATION RATE OF *Bombyx mori* SILK FIBROIN
THROUGH GAMMA RADIATION FOR BIOMEDICAL APPLICATIONS)

อมรเทพ คชคุ้ม 4736139 EGBE/M

วศ.ม. (วิศวกรรมชีวการแพทย์)

คณะกรรมการควบคุมวิทยานิพนธ์ : บวรลักษณ์ อุนคานนท์, Ph.D. (Chemical Engineering),
รัชনীย์ อุดมแสงเพชร, Ph.D. (Immunology)

บทคัดย่อ

เส้นไหมถูกนำมาใช้งานด้านชีวการแพทย์นานนับศตวรรษ โดยเฉพาะอย่างยิ่งไหมเย็บแผลซึ่งผลิตได้จากเส้นใยของรังไหมที่หนอนไหมสร้างขึ้น ไหมเป็นเส้นใยโปรตีนธรรมชาติที่มีความแข็งแรงที่สุด ซึ่งประกอบด้วยแกนไฟโบรอิน 2 แกนห่อหุ้มด้วยกาวไหมที่เรียกว่า เซรีซิน ทั้งนี้เส้นไหมธรรมชาติก่อให้เกิดปัญหาเกี่ยวกับความเข้ากันได้กับระบบภูมิคุ้มกันของร่างกายมาช้านานซึ่งอาจเกิดจากสารเซรีซินที่ตกค้างอยู่บนเส้นไหม นอกจากนี้พบว่ามีกรดอะมิโนในผู้ป่วยบางรายถึงแม้ว่าจะได้กำจัดสารเซรีซินไปแล้ว ซึ่งกรณีนี้น่าจะมีสาเหตุมาจากการสลายตัวที่ช้าเกินไปของเส้นไหม ดังนั้นจึงได้มีการพยายามลดเวลาการสลายตัวของเส้นไหมเพื่อให้ไหมสามารถย่อยสลายตัวได้เร็วขึ้นโดยใช้การฉายรังสีแกมมาเข้าช่วย

เส้นไหมจากไหมพันธุ์ไทยพื้นบ้านพันธุ์นางน้อยศรีสะเกษ-1 ได้ถูกนำมาใช้ในการศึกษาเส้นไหมถูกนำมาฉายรังสีที่ความเข้มของรังสีต่างๆกันก่อนจะนำไปทดสอบการสลายด้วยเอนไซม์โปรตีเอส ผลการทดลองพบว่าอัตราการสลายตัวของเส้นไหมเพิ่มขึ้นตามปริมาณรังสีที่เพิ่มขึ้น ซึ่งการสลายตัวนี้สามารถวัดได้จากการลดลงของความแข็งแรงของพันธะเปปไทด์ การลดลงของโครงสร้างผลึก น้ำหนักของเส้นไหมที่ลดลง การมีรอยแตกเพิ่มขึ้นบนเส้นไหม และการปล่อยกรดอะมิโนที่มีโครงสร้างเป็นวงแหวนและโปรตีนขนาดเล็กออกมาในสารละลายที่ได้จากการสลายตัวของเส้นไหมถึงแม้ว่าการฉายรังสีจะช่วยทำให้เส้นไหมสลายตัวเร็วขึ้น แต่ก็ทำให้ความสามารถในการเกาะของเซลล์บนเส้นไหมลดลงเมื่อใช้ปริมาณรังสีที่สูง นอกจากนี้ได้มีการทดสอบความเข้ากันได้ของร่างกายเบื้องต้นโดยทดสอบการตอบสนองต่อเม็ดเลือดขาว ซึ่งพบว่าไม่มีการตอบสนองจากเซลล์เม็ดเลือดขาวต่อไฟโบรอิน ซึ่งแสดงถึงความปลอดภัยในการใช้ในร่างกาย และสามารถยืนยันได้ว่าเส้นไหมพันธุ์ไทยมีคุณสมบัติที่สามารถนำไปพัฒนาเป็นวัสดุใช้ในทางชีวการแพทย์ต่อไปได้

CONTENTS

	Page
ACKNOWLEDGEMENT	iii
ABSTRACT	iv
LIST OF TABLES	ix
LIST OF FIGURES	x
LIST OF ABBREVIATIONS	xiv
CHAPTER	
I INTRODUCTION	
1. Background	1
2. Objective	2
3. Scope of study	2
II LITERATURE REVIEW	
1. Silkworm silk	3
2. <i>Bombyx mori</i> var. <i>Nangnoi Sisaket-1</i>	4
3. Structure of silk fiber	5
4. Properties of silk fiber	7
5. Biocompatibility of silk	8
6. Utility of silks in biomedical applications	9
6.1 Suture silks	10
6.2 Scaffolds for tissue engineering	10
6.3 Silk powder for scaffold modification	12
7. Gamma rays	13
8. Theory of degradation	17
9. Biodegradation of silk in human body	17
10. Examinations of degradation	18
10.1 Fourier transform infrared spectroscopy	18

CONTENTS (continued)

	Page
10.2 Spectrophotometry	21
10.3 Gel electrophoresis	21
10.4 Scanning electron microscopy	22
10.5 Weight loss measurement	22
11. Related works of silk degradation	23
11.1 Arai et. al., 2004	23
11.2 Horan et. al., 2005	24
11.3 Li et. al., 2003	26
11.4 Sampaio et. al., 2005	27
11.5 Tsuboi et. al., 2001	28
11.6 Shoa et. al., 2005	29
11.7 Pewlong et. al., JAERI Conference 2000-2003	30
III MATERIALS AND METHODS	
1. Materials	32
2. Methods	33
2.1 Silk degumming	33
2.2 Fibroin film preparation	33
2.3 Gamma irradiation	33
2.4 In vitro biodegradation test	33
2.5 Test of cell growth	34
2.6 In vitro white blood cell activation test	34
2.7 Fourier transform infrared spectroscopy	34
2.8 Spectrophotometry	35
2.9 Gel electrophoresis	35
2.10 Scanning electron microscopy	35

CONTENTS (continued)

	Page
IV RESULTS	
1. Effect of radiation on silk fibroin	36
2. In vitro biodegradation test	39
3. Effect of irradiation on cell growth	44
4. In vitro white blood cell activation test	46
V DISCUSSION	49
VI CONCLUSION	54
REFERENCES	55
APPENDIX	58
BIOGRAPHY	67

LIST OF TABLES

	Page
Table 2.1 Amino acid compositions of <i>Bombyx mori</i> fibroin and sericin	6
Table 2.2 Comparison of mechanical properties of silk fiber to several types of biomaterial fibers and tissues commonly used today	7
Table 2.3 Biological responses to virgin silk fibers	8
Table 2.4 Examples of silk's utility as a matrix material in tissue engineering	11
Table 2.5 Characteristic infrared absorption frequencies	19
Table 2.6 Weight loss of silk fibroin	23
Table 2.7 Specific peptide bonds of enzymatic digestion	24
Table 2.8 Amino acid composition (g/100 g) of degradation products of porous silk fibroin sheets exposed to protease XIV	27
Table 4.1 Peak areas of Amide I, Amide II, Amide III, and Amide I per Amide II of silk fibroin at different irradiation doses	37
Table 4.2 Weight loss percentages of irradiated silk fibroin incubated in 1 mg/ml protease in 7, 14, 21 and 28 days	39
Table 4.3 Peak areas of Amide I, Amide II, Amide III, and Amide I per Amide II of irradiated silk fibroin treated by PBS for 28 days	42
Table 4.4 Peak areas of Amide I, Amide II, Amide III, and Amide I per Amide II of irradiated silk fibroin treated by 1 mg/ml protease for 28 days	42
Table 4.5 Measurement of optical density at 280 nm of degradation products incubated in PBS (control) and 1 mg/ml protease for different times	43
Table 4.6 Amounts of cell growth on irradiated silk fibroin fibers	46

LIST OF FIGURES

	Page
Figure 2.1 (A), cultivated cocoons (<i>B. mori</i>): (B), wild cocoon (<i>A. pernyi</i>)	3
Figure 2.2 <i>Bombyx mori</i> silkworms	4
Figure 2.3 <i>Bombyx mori</i> var. <i>Nangnoi Sisaket-1</i> cocoon	5
Figure 2.4 Structure of silk fiber	6
Figure 2.5 β -sheet structure in polypeptide chains of silk fibroin	6
Figure 2.6 Processes of making 3 forms of silks used for biomedical applications	9
Figure 2.7 A helical wire-rope scaffold for ACL reconstruction	12
Figure 2.8 The hBMSCs after 30 minutes of seeding on scaffolds	12
Figure 2.9 The hBMSCs after 14 days of cultivation on scaffold	12
Figure 2.10 PCL-scaffold surface	13
Figure 2.11 Modified PCL-scaffold surface (PCL + fibroin)	13
Figure 2.12 Electromagnetic spectrum	14
Figure 2.13 Penetrating properties of alpha, beta and gamma rays to many kinds of materials	14
Figure 2.14 Gamma irradiator	16
Figure 2.15 Schematic illustration of phagocytosis	18
Figure 2.16 Basic structure of protein	20
Figure 2.17 Vibrational responses of Amide I, Amide II, and Amide III	20
Figure 2.18 FT-IR spectrum of silk fibroin (<i>Bombyx mori</i> var. <i>Nangnoi Sisaket-1</i>) with the characteristic bands	20
Figure 2.19 Structures of aromatic amino acids	21
Figure 2.20 FT-IR spectra of silk fibroin incubated in 1.0 mg/ml protease for (A) 1 day, (B) 21 days, (C) 42 days or (D) 70 days	25

LIST OF FIGURES (continued)

	Page
<p>Figure 2.21 Gel electrophoresis of silk fibroin (Commassie Blue staining): molecular weight marker (lanes 1 and 9), reduced laminin (lane 2), silk incubated in 1.0 mg/ml protease for 1 day (lane 3), 21 days (lane 4), 70 days (lane 5), or in PBS for 1 day (lane 6), 21 days (lane 7), and 70 days (lane 8)</p>	25
<p>Figure 2.22 SEM images of silk fibers incubated in PBS for 1 day (a), 21 days (b), 42 days (c), and in 1.0 mg/ml protease solution for 1 day (d), 21 days (e) and 42 days (f)</p>	26
<p>Figure 2.23 FT-IR spectra of silk fibroin without mushroom tyrosinase (a), with 0.38 U/mg mushroom tyrosinase (b), with 0.72 U/mg mushroom tyrosinase (c), and with 3.3 U/mg mushroom tyrosinase (d)</p>	28
<p>Figure 2.24 FT-IR spectra changes of silk fibroin: A spectrum of neat fibroin film with random coil structure (a), after a thermal treatment at 470 K (b), after 266 nm irradiation (c), and commercially supplied fibroin whose secondary structure was of mixed type of β-sheet and random coil structures</p>	29
<p>Figure 2.25 FT-IR spectra of non-irradiated silk (lower curve), and UV/ozone irradiated silk for 40 min (upper curve)</p>	30
<p>Figure 2.26 Tensile strength of irradiated silk fibroin fibers</p>	30
<p>Figure 2.27 Effect of radiation on solubility of silk fibroin fibers in distilled water</p>	31
<p>Figure 4.1 Appearance of silk fibroin fibers after gamma irradiation: unirradiated fibers (a), 100 kGy (b), 500 kGy (c), and 1000 kGy (d)</p>	36
<p>Figure 4.2 SEM images of silk morphology after gamma irradiation: unirradiated fibers (A), and 600 kGy (B)</p>	36
<p>Figure 4.3 FT-IR spectra of irradiated silk fibroin: 0 kGy (black), 1000 kGy (blue), 1500 kGy (red), 2000 kGy (green) and 3000 kGy (brown)</p>	37
<p>Figure 4.4 Crystallinity degree of silk fibroin at various irradiation doses</p>	38

LIST OF FIGURES (continued)

	Page
Figure 4.5 Water dissolution of silk fibroin film at various irradiation doses	38
Figure 4.6 Degradation products of irradiated silk fibroin (0, 100, 500 and 1000 kGy from left to right, respectively) for 28 days: (A) is control, (B) is in 1 mg/ml protease.	39
Figure 4.7 SEM images of irradiated silk fibroin incubated in PBS (control): 0 kGy (A), 100 kGy (B), 500 kGy (C) and 1000 kGy (D), and in 1 mg/ml protease for 28 days: 0 kGy (E), 100 kGy (F), 500 kGy (G) and 1000 kGy (H)	40
Figure 4.8 FT-IR spectra of irradiated silk fibroin incubated in PBS (control) for 28 days: 0 kGy (black), 100 kGy (blue), 500 kGy (red) and 1000 kGy (green)	41
Figure 4.9 FT-IR spectra of irradiated silk fibroin incubated in 1 mg/ml protease for 28 days: 0 kGy (black), 100 kGy (blue), 500 kGy (red) and 1000 kGy (green)	41
Figure 4.10 Spectrophotometry analysis of 1 mg/ml protease incubated for 7 days (black), 14 days (blue), 21 days (red) and 28 days (green)	43
Figure 4.11 Gel electrophoresis of degradation products: molecular weight marker (lane 1), 1 mg/ml protease (lane 2), control conditions of unirradiated sample (lane 3), 100 kGy (lane 4), 500 kGy (lane 5), 1000 kGy (lane 6), enzymatic conditions of unirradiated sample (lane 7), 100 kGy (lane 8), 500 kGy (lane 9) and 1000 kGy (lane 10)	44
Figure 4.12 Fibroblasts grow on irradiated fibroin fibers (3 days of culturing).	45
Figure 4.13 Fibroblasts grow on irradiated fibroin fibers (7 days of culturing).	45
Figure 4.14 Blank fibroin film with non-activation of white blood cells (60 min of incubation time, 40X)	46

LIST OF FIGURES (continued)

	Page
Figure 4.15 White blood cell activation to the fibroin film growing with fibroblasts incubated in different times (15, 30, 45, 60, 120 and 180 min). Blue-color cells were neutrophils and the transparent cells were monocytes.	47
Figure 4.16 White blood cell count on activated fibroin films (film + fibroblast) incubated in different times. Monocyte count (upper curve) and neutrophil count (lower curve)	48

LIST OF ABBREVIATIONS

%	percent
α	alpha
β	beta
ϵ	epsilon
γ	gamma
ACL	anterior cruciate ligament
Ala	alanine
Arg	arginine
Asp	aspartic acid
$^{\circ}\text{C}$	degree Celsius
$\text{CaCl}_2 \cdot 2\text{H}_2\text{O}$	calcium chloride dihydrate
$\text{C}_2\text{H}_5\text{OH}$	ethanol
cm	centimeter
cm^{-1}	per centimeter
CO_2	carbon dioxide
${}^{60}_{27}\text{Co}$	Cobalt-60
Cys	cysteine
$e^{-1}, {}^0_{-1}e$	electron
$e^{+1}, {}^0_{+1}e$	positron
e.g.	for example
et. al.	and other people
etc.	and other things
ETO	ethylene oxide
FDA	Food and Drug Administration
FT-IR	Fourier Transform Infrared Spectroscopy
g	gram

LIST OF ABBREVIATIONS (continued)

Gly	glycine
Gpa	gig Pascal
hr	hours
H	hydrogen
His	histidine
H ₂ O	water
hBMSC	human bone marrow stromal cells
i.e.	that is
IgE	immunoglobulin type E
IgG	immunoglobulin type G
Ile	isoleucine
K	Kelvin
KBr	potassium bromide
kDa	kilo Dalton
keV	kilo electron volts
kg	kilograms
kGy	kilo Grays
Leu	leucine
Lys	lysine
m	moderate frequency band
Met	methionine
mg	milligram
ml	milliliter
min	minutes
mm ²	square millimeter
Mpa	mega Pascal
MWCO	molecular weight cut off
n	neutron
nm	nanometer

LIST OF ABBREVIATIONS (continued)

NMR	nuclear magnetic resonance
Na ₂ CO ₃	sodium carbonate
⁶⁰ ₂₈ Ni	Nickel-60
⁶⁰ ₂₈ Ni*	excited Nickel-60
O.D.	optical density
p	proton
PBS	phosphate buffered saline
PCL	poly ε-caprolactone
PDS	polydioxanone
PGA	polyglycolic acid
Phe	phenylalanine
PLA	polylactic acid
poly-HEMA	poly-2-hydroxyethyl methacrylate
Pro	proline
rpm	round per minute
RPMI	Roswell Park Memorial Institute
sec	second
SEM	Scanning Electron Microscopy
Ser	serine
Thr	threonine
Try	tryptophan
Tyr	tyrosine
U	unit
USP	United States Pharmacopeia
UTS	ultimate tensile strength
UV	ultraviolet
μl	micro liter
v	variable frequency band

LIST OF ABBREVIATIONS (continued)

ν_e	neutrino
$\bar{\nu}_e$	anti-neutrino
Val	valine
<i>var.</i>	variety
W_i	initial weight
W_p	post weight

CHAPTER I

INTRODUCTION

1. Background

Silks are generally defined as continuous protein fibers produced by some Lepidoptera larvae such as silkworms, spiders, scorpions, and mites to form their cocoons [1]. The most extensively characterized silks are produced from *Bombyx mori* silkworms. These protein fibers are known as the strongest natural protein fiber which well known in textile quality, the silkworm silk is so called “The Queen of Fibers”.

Normally, people know the silks as textile materials, because they have been used to fabricate garments for over 4,000 years [2]. Whereas, the utilization of silks in biomedicine have been occurred recently. In fact, the first biomedical application of silks is only for suture due to its good mechanical properties and can be gradually degraded in vivo within 2 years [1]. During the past 20 years, there have been some reports about biocompatibility problems caused by silkworm silks, which were recently discovered that the biocompatibility problems were caused by the contamination from residual sericin (silk gum) [1, 3, 4, 5]. Therefore, to prevent an adverse effect that might be occurred to the patients, the sericin must be removed before utilizing the silks in biomedicine.

Although the sericin is entirely removed, the biocompatibility problems may be occurred in some patients. In some cases, residues of silk fibroin after the completed surgery can become the allergic-like proteins which can induce the host immune responses [1]. From these problems, the prolong biodegradability of silks might be one of the causes. Thus, an attempt to reduce the degradation period of silk fibroin through radiation is then studied.

2. Objective

The purpose of this study is to investigate the biodegradation rate of Thai silk fibroins through gamma irradiation, which can be involved for developing and designing the resorbable silk-based biomedical materials used for various biomedical purposes in the future.

3. Scope of study

The scope of this study includes:

1. Degumming of silk fibers using Thai local silkworm silks, *Bombyx mori* var. *Nangnoi Sisaket-1*.
2. Effect of radiation intensity on the biodegradation rate of silk fibroin fibers.
3. Effect of radiation intensity on the capability of cell attachment and cell growth on silk fibroin fibers.
4. In vitro preliminary study of biocompatibility of silk fibroin to human white blood cells.

CHAPTER II

LITERATURE REVIEW

1. Silkworm silk

As mentioned earlier, silk from silkworms is the strongest natural animal fiber. The length of silk filament is approximately 900-1,700 meters with 9-11 microns in diameter [2]. Silk proteins are produced within specialized glands of silkworm after biosynthesis in epithelial cells, then followed by secretion into the lumen of these glands where the proteins are stored prior to spinning into fibers to form cocoons (Figure 2.1). In fact, there are five species of silkworm in the world:

1. *Bombyx mori* (Mulberry silkworms)
2. *Antheraea mylitta* (Tasar silkworms)
3. *Antheraea pernyi* (Oak-tasar silkworms)
4. *Antheraea assamensis* (Muga silkworms)
5. *Philosamia ricini* (Eri silkworms)

Bombyx mori is sometimes called “cultivated silkworms”. Their fibers are fine, almost white and soft with luster after degumming processes – sericin removing processes. While *Antheraea mylitta*, *Antheraea pernyi*, *Antheraea assamensis* and *Philosamia ricini* can be categorized as “wild silkworms”. The appearances of wild silk fibers are coarse, irregular, lusterless and brownish. Moreover, after the degumming processes the wild silks are never as white as the cultivated silks. Therefore, the *Bombyx mori* is more popular for sericulture – cultivation of silkworms – than the others.



(A)



(B)

Figure 2.1 (A), cultivated cocoons (*B. mori*): (B), wild cocoon (*A. pernyi*)

Thai silk is one of the mulberry silkworm silks but differs than the others in appearances, i.e. more yellowish in color (European cocoon is white), coarser filaments, and contains more sericin (up to 38%) than normal mulberry silk (20-25%) [2]. Thailand is abundant in sericulture, especially in the northern and north-eastern parts of the country due to the climates advantage, which are suitable for sericulture. There is a clear study showed that the different climates will affect the quality and quantity of silk fibers (difference in the protein-based structures of silk fiber), which cause the differences in their mechanical properties including the degradability of silk fiber. Generally, there are several varieties of Thai silkworms, but only few varieties are guaranteed by the Department of Agriculture, Thailand, in their fiber qualities and the stability of their breeds, for examples *Bombyx mori* var. *Nangnoi Sisaket-1*, var. *Dokbua*, var. *Luangkoraj*, var. *Ubonrajthanee-60*, etc. [6]. In this experiment, silks from *Bombyx mori* var. *Nangnoi Sisaket-1* are chosen for the study.

2. *Bombyx mori* var. *Nangnoi Sisaket-1*

Bombyx mori var. *Nangnoi Sisaket-1* is a thoroughbred Thai-native silkworm. According to the climate endurance and easy for sericulture, they are widely cultivated in almost parts of Thailand. The *Bombyx mori* var. *Nangnoi Sisaket-1* has been guaranteed by the Department of Agriculture, Thailand, since 19 December 1988 [6]. Some characteristics of this breed are shown as follows:

1. Silkworms are ivory white without any spots (Figure 2.2).
2. Silkworm age is 18-22 days.
3. One female moth contains about 348 eggs.
4. Polyvoltine breed (more than two generations per year).
5. High-temperature resistance for cultivation (33-35 °C).
6. Yellow spindle-shaped cocoon with 1.5×3.0 cm of size (Figure 2.3).



Figure 2.2 *Bombyx mori* silkworms



Figure 2.3 *Bombyx mori var. Nangnoi Sisaket-1* cocoon

7. Average weight of fresh cocoon is 0.96 gram.
8. Length of silk fiber per a cocoon is approximately 370-410 meters.
9. Size of silk fiber is 2.5 deniers – weight in gram of 9,000 meters.

3. Structure of silk fiber

Silk fiber composes of two major proteins; fibroin and sericin, which consisted of two fibroin cores coated with sericin (Figure 2.4). Both fibroin and sericin constitutes of the same amino acids (18 amino acids) but difference in their amounts as shown in Table 2.1. Fibroin or silk core is a major component of silk fiber (75% of silk fiber). It contains at least two fibroin proteins, light chain (25 kDa) and heavy chain (325 kDa) [7]. Sericin or silk gum is a minor component of silk fiber (25% of silk fiber). It is brittle and inelastic that conceals the unique luster of fibroin. Another different property between the fibroin and sericin is the crystallinity, which can be found only in fibroin. The fibroin contains repetitive amino acids (-Gly-Ala-Gly-Ala-Gly-Ser-) along its sequence forming a large number of β -sheet microcrystallites (Figure 2.5), which act as a reinforcement and contribute to the strength and stiffness of the silk [8, 9]. On the other hand, the sericin is amorphous and acts as an adhesive binder to maintain the structural integrity of the cocoon. Due to the high degree of crystallinity, the high molecular weight of polypeptide chains, the intensive hydrogen bonding between carboxyl groups and amino groups, the fibroin is water insoluble. In contrast, the sericin is amorphous structure with low molecular weight of polypeptide chains. Therefore, the sericin can be dissolved in hot water and alkaline solution [10].

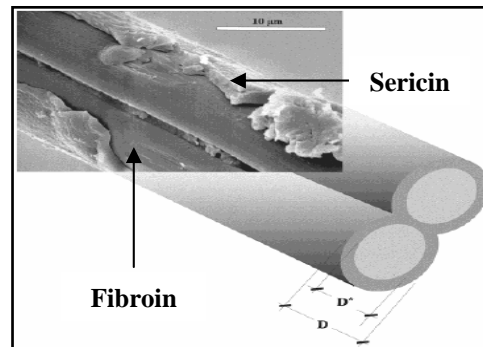


Figure 2.4 Structure of silk fiber [8]

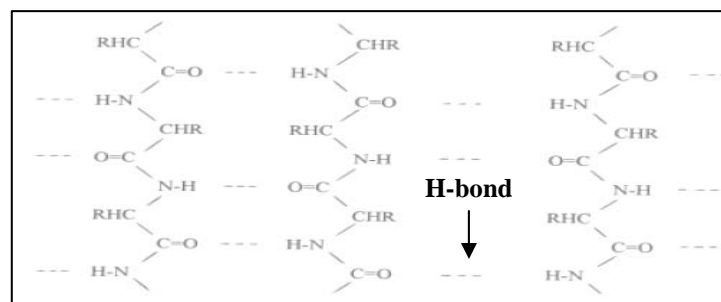


Figure 2.5 β -sheet structure in polypeptide chains of silk fibroin [2]

Table 2.1 Amino acid compositions of *Bombyx mori* fibroin and sericin [2]

Amino acids	Fibroin (%)	Sericin (%)
Glycine	44.60	12.70
Alanine	29.40	5.51
Valine	2.20	2.68
Leucine	0.53	0.72
Isoleucine	0.66	0.55
Serine	12.10	31.97
Threonine	0.91	8.25
Aspartic acid	1.30	13.84
Glutamic acid	1.02	5.80
Lysine	0.32	3.26
Arginine	0.47	2.86
Histidine	0.14	1.30
Tyrosine	5.17	3.40
Phenylalanine	0.63	0.43
Proline	0.36	0.57
Tryptophan	0.11	0.01
Methionine	0.10	0.05
Cysteine	0.20	0.14

4. Properties of silk fiber

Silk fibers are extremely strong. A filament of silk is stronger than an equal diameter filament of steel [11]. Silk fibers are insoluble in most organic solvents, including water, dilute acid, and alkaline. They are biodegradable and biocompatible materials, which are suitable for utilizing as biomaterials. Furthermore, the silk fibers resist failure in compression, stabilize at physiological temperature, and maintain the mechanical tensile integrity in vitro in tissue culture conditions [12]. Some mechanical properties of silk fiber are shown in Table 2.2.

Table 2.2 Comparison of mechanical properties of silk fiber to several types of biomaterial fibers and tissues commonly used today [1]

Materials	UTS (Mpa)	Modulus (Gpa)	Strain at break (%)
Silkworm silk (with sericin)	500	5-12	19
Silkworm silk (without sericin)	610-690	15-17	4-16
Collagen	0.9-7.4	0.0018-0.046	24-68
PLA	28-50	1.2-3.0	2-6
Tendon	150	1.5	12
Bone	160	20	3

5. Biocompatibility of silk

As mentioned earlier, there are some reports during the past 20 years in biocompatibility problems of biomedical suture silks. However, the recent studies [3,4] reveal that these problems are occurred due to the residual sericin coating on the suture silk fibers. The comparison between the virgin and black braided silks (see 6.1) in biocompatibility shows that the virgin silk is a potential allergen causing an immune response and hypersensitivity (Type I and IV) [1]. These occurrences are caused by sericin in the virgin silk. According to Wen et. al. [3], the extracted sericin was responsible for sensitization (the development of a T-cell mediated allergic response) by skin testing of 64 children with asthma. Furthermore, Zaoming et. al. [4] concluded that the IgEs were produced in response to the sericin causing the allergic responses, clarifying the role of these fibroin contaminants as the main allergenic agent in silk. Therefore, all silk fibers should be free from sericin by degumming process before utilizing in vivo to prevent the biological responses that might occurred to the patients. The biological responses to virgin silks are summarized in Table 2.3.

Table 2.3 Biological responses to virgin silk fibers [1]

Types of silk	Responses	In vivo or in vitro model / tissue site
Virgin	- Acute and chronic inflammation initially including conjunctival and episcleral hyperemia progressing to chemosis and nodular episcleritis, peripheral corneal ulceration and wound necrosis.	Human / ocular cataract surgery
	- Sensitization to virgin silk during bilateral cataract surgery following the use of virgin silk on the first eye.	
	- Delayed hypersensitivity to virgin silk resulting in asthma.	Children <15 year old / skin tests

Table 2.3 Biological responses to virgin silk fibers (continued)

Types of silk	Responses	In vivo or in vitro model / tissue site
Virgin	- IgE obtains from sera isolated from 8 of 9 patients with allergy to silk bound specifically to sericin and was negative towards fibroin.	In vitro immunoblot of IgE and IgG isolated from sera of 9 persons allergic to silk
Black braided	No reactions to the silk.	Human / ocular cataract surgery.

6. Utility of silks in biomedical applications

During the decades of using silks as biomedical materials, some questions about biocompatibility and biological responses to silk fibers have raised. The recent studies show that the sericin is a major cause of adverse problems with biocompatibility and hypersensitivity to the silks. If sericin is removed, the biological responses to the fibroin cores appear to be compatible. Furthermore, there are clear evidences that silks are susceptible to proteolytic degradation in vivo over a longer period of time. Due to the properties of silk in biocompatibility and biodegradation, silks are utilized for biomedical applications in many ways, for examples sutures, scaffolds for tissue engineering, and artificial cornea. There are 3 forms of silks commonly used in biomedicine: fibers, films and powder (Figure 2.6).

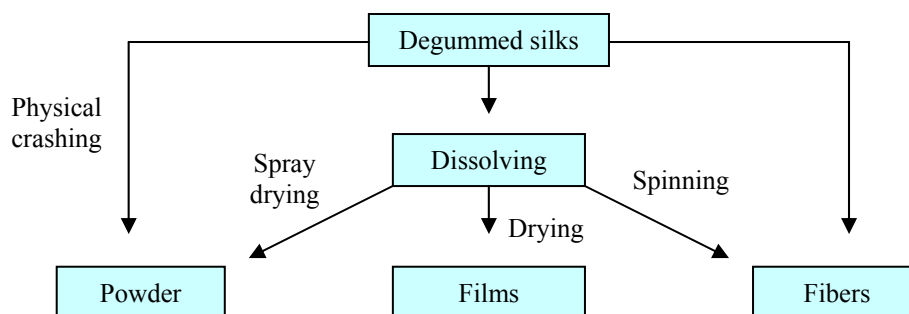


Figure 2.6 Processes of making 3 forms of silks used for biomedical applications [13]

6.1 Suture silks

Silk fibers have been used most extensively as suture materials for wound ligation, thereafter it becomes the most common natural suture used in medicine over the centuries. In fact, it is the first biomedical application of silk fibers. The processes of suture silks in industry were started by degumming of sericin from virgin silks. As suture silks, the fibroin fibers are usually coated with waxes or silicone to enhance material properties and reduce fraying, these suture silks are commonly referred to as “black braided silks” [1]. The black braided silk occurred in the late 1970 and early 1980 [1].

During the past 20 years, a wide variety of biodegradable synthetic materials have dominated the suture market, for examples polyglycolic acid (PGA), polydioxanone, polyglyconate, etc. These polymers are absorbed and lose their tensile strength within 2-3 months [14], which are faster than those of silks whose tensile strength will lose within 2 years. Generally, suture materials should be strong, handle easily, and form secure knots, thus they require the following characteristics for general surgical applications [1]:

1. Tensile strength – to match the clinical repair.
2. Knot strength – the amount of force required to cause a knot to slip.
3. Elasticity – the ability to conform to the current stage of wound repair.
4. Degradability – ability to be metabolized by the host once its repair function has been completed.
5. Memory – change in stiffness over time. The better suture is less memory.
6. Tissue Reactivity – non-irritant.
7. Free from infection – related to the material’s geometry, e.g. multifilament versus monofilament.

6.2 Scaffolds for tissue engineering

Tissue engineering has increased the demand as biomaterial matrix to support the development of tissues in vitro prior to in vivo implantation. The matrix or scaffold plays an important role in communicating or transferring between the local environment and the cells seeded within or on the scaffold. The scaffold must support cell attachment, spreading, growth and differentiation. It will be advantageous if the

matrix degrades into biocompatible fragments or monomers capable of being metabolized by host cells. However, the degradation rate must at least equivalent to the rate of tissue growth and development in order to optimize the functionality of the scaffolds. A mismatch in these rates can lead to premature failure of the tissue. Silk fibroin offers the versatility in scaffold design for a number of tissue engineering needs in which mechanical properties and biological interactions are major factors for success. The silk fibroin can be fabricated as cellular supporting matrix in many forms (e.g. foams, films, fibers, tubes and meshes), which depend on cell types for ingrowth and the final targets of tissue differentiation, instances ligament, tendon, bone, cartilage, and blood vessel.

There are many reports claiming that the silk fibroin is a suitable material for being cellular supporting scaffolds: Inouye et. al. [15] demonstrated that the silk fibroin film can be used as a matrix for animal cell cultivation; Minoura et. al. [16] showed that the extracted fibroin is a suitable matrix for cell and tissue culture; and Altman et. al. [12] was successful in making silk fibroin scaffolds for anterior cruciate ligament (ACL) reconstruction. Some utilities of silk fibroin as a matrix in tissue engineering are shown in Table 2.4.

Table 2.4 Examples of silk's utility as a matrix material in tissue engineering [1]

Silk forms	Supported cell type in vitro	Authors
Fibroin films	SE1116 (human colon adenocarcinoma); KB (human mouth epidermoid carcinoma); QG56 (human lung carcinoma)	Inouye et. al.
Fibroin films	Mouse fibroblasts	Minoura et. al.
Fibroin fibers	hBMSC (human bone marrow stromal cells); human adult anterior cruciate ligament fibroblasts	Altman et. al.

Silk scaffold for ACL reconstruction is another application of silk fibroin fibers that is deemed to be successful to help the patients who suffering from ACL ruptures. This is an accomplishment of Gregory Altman in using the natural protein fiber like silks instead of degradable polymers for ACL scaffold fabrication. A helical wire-rope scaffold (Figure 2.7) exhibits the mechanical properties similar to a human ACL. Moreover, this scaffold acts as a good matrix for cell growth and differentiation (Figures 2.8 and 2.9).

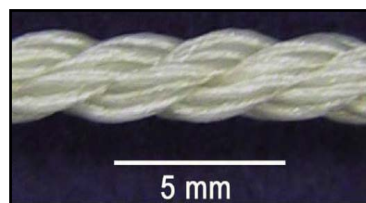


Figure 2.7 A helical wire-rope scaffold for ACL reconstruction [1]

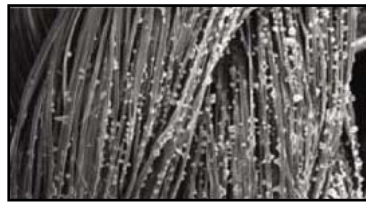


Figure 2.8 The hBMSCs after 30 minutes of seeding on scaffolds [1]



Figure 2.9 The hBMSCs after 14 days of cultivation on scaffold [1]

6.3 Silk powder for scaffold modification

Due to the biodegradable, biocompatible, and cell adhesive properties of silks, silk powder can be mixed with polymers to modify scaffolds to get both characteristics of silk and polymer. Chen et. al. [17] modified the PCL (poly ϵ -caprolactone) scaffold by mixing with silk fibroin powder to improve the biocompatible property of PCL. They found that the fibroin powder was not only

improving the biocompatibility, but also increased the porous surfaces of the scaffold for cell attachment. The porous surfaces of the PCL and the PCL mixed with fibroin powder scaffolds are shown in Figures 2.10 and 2.11 respectively.

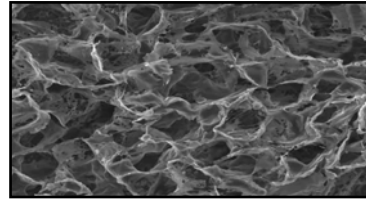


Figure 2.10 PCL-scaffold surface [17]

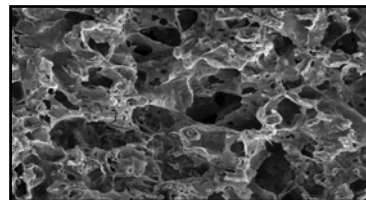


Figure 2.11 Modified PCL-scaffold surface (PCL + fibroin) [17]

7. Gamma rays

Gamma rays (γ -rays) are an energetic form of electromagnetic radiation produced by radioactive decay [18]. Gamma radiation is a form of ionizing radiation producing the highest energy, which their photons have about 10,000 times as much energy as the photons in the visible range of the electromagnetic spectrum (Figure 2.12). Gamma photons have no mass and no electrical charge, so they are pure electromagnetic energy [19]. The gamma rays are defined to begin at the energy of 10 keV. Although the electromagnetic radiation from 10 keV to several hundred keV is also referred to as hard X-rays, there is no physical difference between gamma rays and X-rays of the same energy. The gamma rays are distinguished from X-rays by their origins. Gamma ray is a term for high-energy electromagnetic radiation produced by nuclear transitions, while X-ray is a term for high-energy electromagnetic radiation produced by energy transitions due to accelerating electrons [18].

Because of their high energy, the gamma photons travel at the speed of light and can cover hundreds to thousands of meters in air before spending their energy

[19]. They can pass through many kinds of dense materials, including human tissues. Very dense materials, such as lead, are commonly used as shielding to slow or stop the gamma photons (Figure 2.13).

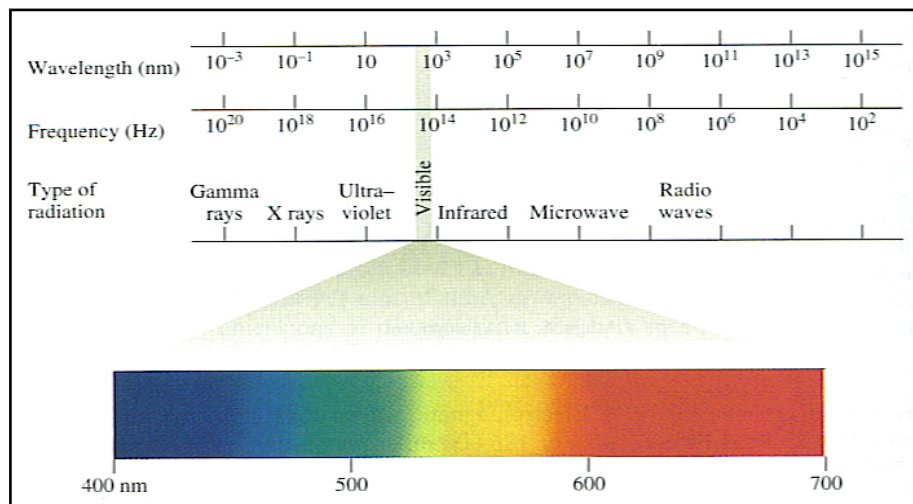


Figure 2.12 Electromagnetic spectrum [18]

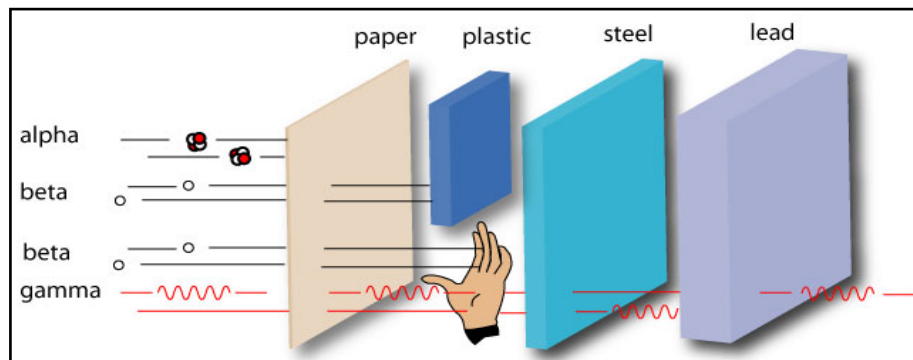


Figure 2.13 Penetrating properties of alpha, beta and gamma rays to many kinds of materials [18]

Gamma rays are often produced alongside other forms of radiation, such as beta decay. An excess of neutrons in an atom's nucleus will make it unstable, then a neutron is converted into a proton. During this process, an electron (e^- or ${}_{-1}^0e$) and an anti-neutrino ($\bar{\nu}_e$) are released, so called beta decay (equation 2.1). When there is an excess of protons in the nucleus, a proton is converted into a neutron in order to make

the nucleus becomes stable. During this process, a positron (e^+ or ${}_{+1}^0e$) and a neutrino (ν_e) are released, called positron decay (equation 2.2). When positrons interact with electrons released from the beta decay process, causing both to be completely destroyed. Two gamma ray photons with the same energy as the mass of the positron and electron are released.



Radionuclides are the most widely used as gamma radiation sources. The penetrating power of gamma photons has many applications. However, while gamma rays are penetrating through materials, they do not make the materials become radioactive [19]. Generally, there are three radionuclides commonly used as gamma emitting sources: Cobalt-60, Cesium-137, and Technetium-99m.

Use of Cobalt-60

1. Sterilization of medical equipments
2. Food pasteurization
3. Cancer treatment
4. Gauge the metal thickness in steel mills

Use of Cesium-137

1. Cancer treatment
2. Investigation of subterranean strata in oil wells
3. Measurement of the liquid flow in numerous industrial processes
4. Measurement of soil density at construction sites
5. Ensure the proper fill level for packages of food, drugs and other products.

Use of Technetium-99m

Technetium-99m is a shorter half-life precursor of Technetium-99. It is widely used for diagnostic studies, such as brain, kidney, bone, liver, spleen, and also blood flow studies.

In this study, the samples are irradiated by Cobalt-60 gamma irradiator (Figure 2.14). Processes of gamma rays produced by Cobalt-60 decay are shown in equations 2.3 and 2.4.

First, Cobalt-60 (${}^{60}_{27}\text{Co}$) decays to excited Nickel-60 (${}^{60}_{28}\text{Ni}^*$) by beta decay:



The ${}^{60}_{28}\text{Ni}^*$ is unstable, so it drops down to the ground state by emitting two gamma rays:



Figure 2.14 Gamma irradiator

8. Theory of degradation

As defined by the United States Pharmacopeia (USP), degradable materials are materials which retain their tensile strength less than 50% within 60 days, if retain more than 50%, they are categorized as non-degradable [1]. Silks can be categorized as non-degradable materials, because they retain greater than 50% of their tensile strength within 60 days of post-implantation in vivo [1, 7]. However, as a protein, silks will be proteolytically degraded and absorbed in vivo over a longer time period.

9. Biodegradation of silk in human body

Biodegradation is a capacity of materials that can be dissolved or digested in a biological system over time. It is a major property of biomaterials, especially scaffolds – porous or fibrous supporting structures which allow cells or tissues for ingrowth. Normally, all biological materials are in vivo absorbed by cellular enzymes. As a protein, silk is also absorbed by protease enzyme produced from the surrounding cells. In fact, the absorption rate depends on the location in the body and the healing process, since these two factors influence the cell population that presented around the material. As mentioned earlier, silk is categorized as a slowly absorbable material composed of crystalline and amorphous regions. The degradation will start in the amorphous regions, and then propagate further to the crystalline regions. In degradation process, silk polypeptide chains are first broken down into smaller fragments. The fragments are then digested by the enzymatic action of white blood cells, this process called “phagocytosis”. In the process of phagocytosis, the white blood cells first ingest the foreign bodies, e.g. a bacterium or fragments of silk fiber. The lysosome granules inside of the cell then secrete enzymes onto the foreign bodies, which are capable of further degrading them into smaller pieces (Figure 2.15). These pieces are eliminated from the body by normal metabolic pathways, such as urine and expiration.

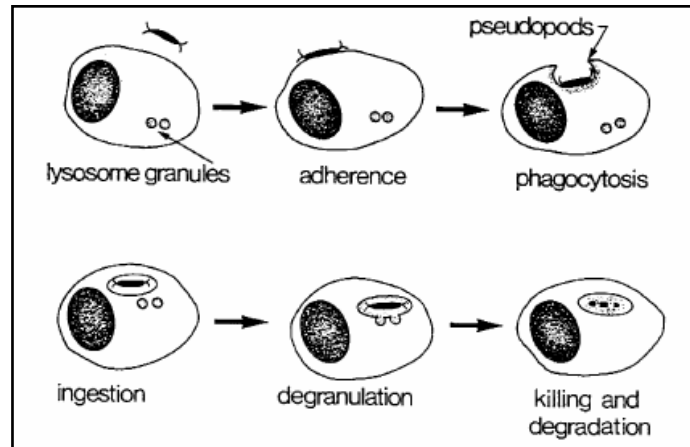


Figure 2.15 Schematic illustration of phagocytosis

10. Examinations of degradation

The degradation of materials can be measured by these factors; decrease in mass, diameter, failure strength, cycles to failure, chemical bonds, and degree of crystallinity. To investigate the degradation in this study, the changes of fibroin structure will be examined by using Fourier transform infrared spectroscopy (FT-IR). Increasing of silk protein in degradation solution after treating with enzyme indicates the degradation of silk fibroin, which can be examined by spectrophotometry and gel electrophoresis. Silk morphology after enzyme digesting can be observed by scanning electron microscopy (SEM). Furthermore, weight loss measurement is used to observe percentages of mass loss after enzyme digestion.

10.1 Fourier transform infrared spectroscopy

Fourier transform infrared spectroscopy (FT-IR) is an analytical technique for material analysis. An infrared spectrum represents a fingerprint of a sample with absorption peaks which correspond to the frequencies of vibrations between the bonds of the atoms making up the material [20]. Because each different material is a unique combination of atoms, no two compounds produce the exact same infrared spectrum. Therefore, infrared spectroscopy can result in a positive identification (qualitative analysis) of every different kind of material. In addition, the size of the peaks in the

spectrum is a direct indication of the amount of material present. Table 2.5 shows some infrared spectrums of individual chemical bonds.

Table 2.5 Characteristic infrared absorption frequencies [21]

Bonds	Compound types	Wavenumbers (cm⁻¹)
C-H	Alkane	2850-2960, 1350-1470
C-H	Alkene	3020-3080 (m), 675-1000
C-H	Aromatic ring	3000-3100 (m), 675-870
C-H	Alkyne	3300
C=C	Alkene	1640-1680 (v)
C≡C	Alkyne	2100-2260 (v)
C=C	Aromatic ring	1500-1600 (v)
C-O	Alcohol, ether, ester, carboxylic acid	1080-1300
C=O	Aldehyde, ketone, carboxylic acid, ester	1690-1760, 1700-1780
O-H	Alcohol, phenol, carboxylic acid	3200-3600 (broad)
N-H	Amine	3300-3500 (m)
C-N	Amine	1360-1800
C≡N	Nitrile	2210-2260 (v)
-NO ₂	Nitro compound	1345-1385

All bands strong unless: m, moderate; v, variable

In protein analysis, the FT-IR provides information about the secondary structure content of proteins, unlike X-ray crystallography and NMR spectroscopy which provide information about the tertiary structure of protein [22]. As mentioned before, each compound has a characteristic set of absorption bands like a fingerprint in its infrared spectrum. Characteristic bands found in the infrared spectra of proteins and polypeptides include the Amide I, Amide II, and Amide III [22]. These arise from the amide bond (peptide bond) that links the amino acids (Figure 2.16). The absorption associated with the Amide I band leads to stretching vibrations of the C=O bond of the amide, the absorption associated with the Amide II band leads to bending vibrations of the N-H bond, and the absorption associated with the Amide III band leads to stretching vibrations of the C-N bond [22, 23] (Figure 2.17).

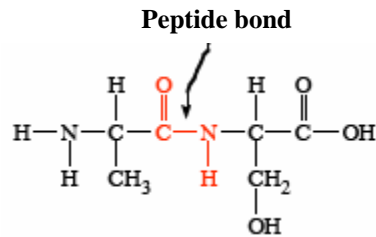


Figure 2.16 Basic structure of protein

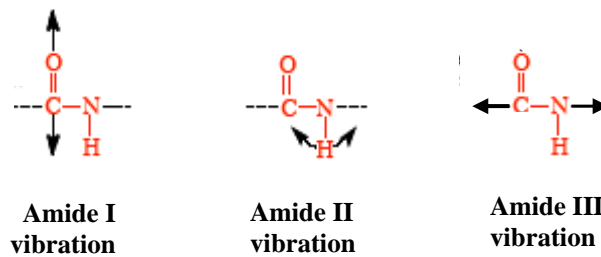


Figure 2.17 Vibrational responses of Amide I, Amide II, and Amide III [22]

Since the structure of silk fibroin is also protein, the degradation of silk fibroin can be investigated by changing of fibroin structure, which can be examined from characteristic bands of silk fibroin, Amide I (1620 cm^{-1}), Amide II (1515 cm^{-1}) and Amide III (1230 cm^{-1}). The characteristic bands of silk fibroin are shown in Figure 2.18.

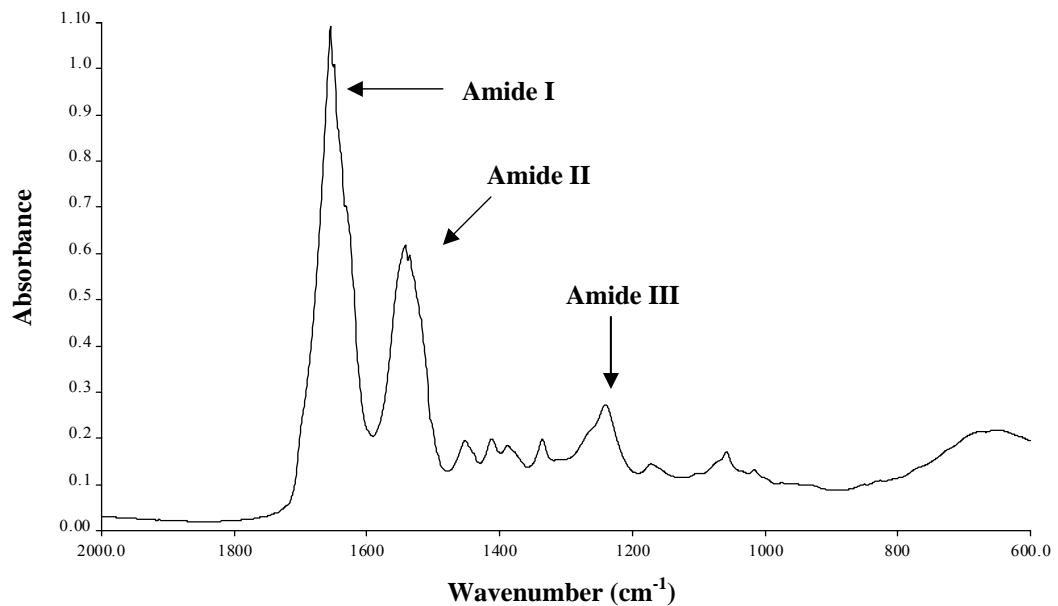


Figure 2.18 FT-IR spectrum of silk fibroin (*Bombyx mori* var. *Nangnoi Sisaket-1*) with the characteristic bands

10.2 Spectrophotometry

Spectrophotometry is an analytical method for measuring amounts of substances based on the absorption of wavelength. In this study, increasing of silk protein in degradation solution can be measured by detecting at wavelength 280 nm, which is specific wavelength absorption of aromatic amino acids – tryptophan, tyrosine and phenylalanine [24, 25], which are found in silk fibroin. The chemical structures of these aromatic amino acids are shown in Figure 2.19.

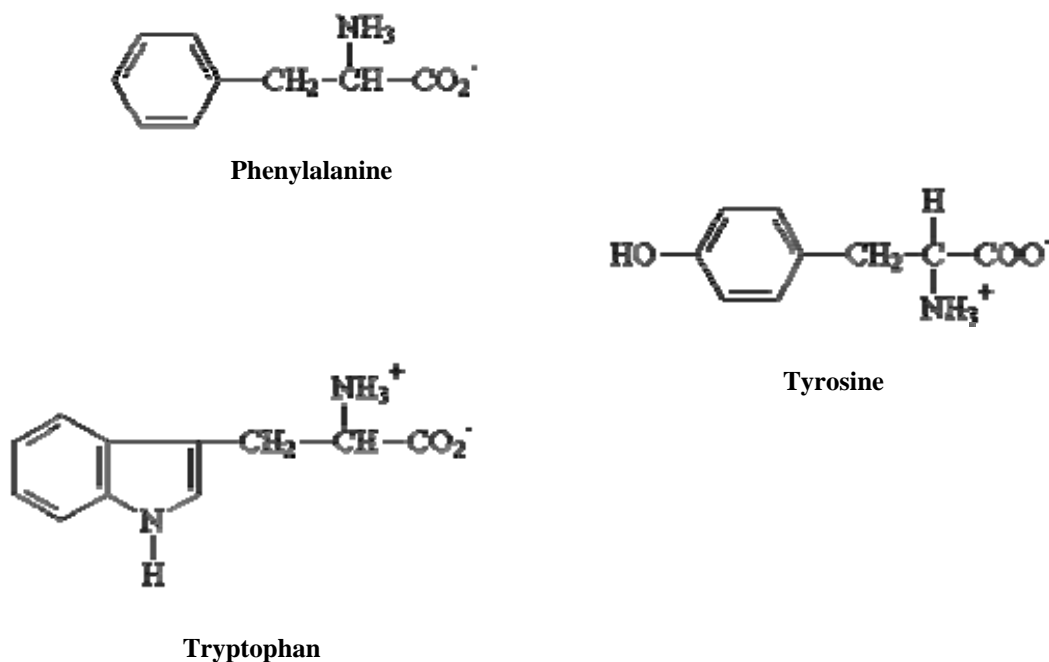


Figure 2.19 Structures of aromatic amino acids

10.3 Gel electrophoresis

Electrophoresis or gel electrophoresis is an analytical method for separating proteins on the basis of size, electrical charge, and other physical properties. A gel is a colloid in a solid form. The term of electrophoresis describes the migration of charged particles under the influence of an electrical field. *Electro* refers to the energy of electricity. *Phoresis*, from the Greek verb *phoros*, means “to carry across”. Therefore, gel electrophoresis refers to a technique that molecules are forced across a span of gel, which is motivated by an electrical current [26]. Comparison to another method for

separating proteins such as chromatography, gel electrophoresis has the advantage that proteins can be visualized as well as separated permitting a researcher to estimate quickly the number of proteins in a mixture or the degree of purity of a particular protein preparation. Also, gel electrophoresis allows determination of crucial properties of a protein such as its isoelectric point and approximate molecular weight.

As mentioned earlier, silk fibroin consists of light chain and heavy chain polypeptides. Therefore, the degradation of silk can be observed by increasing of these proteins in degraded solution, which is displayed on the gel after running electrophoresis. The darkness of the protein bands indicates the amount of protein in solution, which refer to the degradation rate of the silk fibers.

10.4 Scanning electron microscopy

Scanning electron microscopy (SEM) is a method for determining the surface morphology of a solid by measuring the energies of electrons scattered by the atoms on the surface of a sample. In this study, the morphology of degraded silks can be examined by SEM. The surface erosion and the reduction in diameter of silk fibers indicate the degradation of silks.

10.5 Weight loss measurement

Weight loss measurement is another technique to determine the degradation of samples. It can be calculated using equation 2.5:

$$\text{Weight loss (\%)} = \frac{W_i - W_p}{W_i} \times 100 \quad (2.5)$$

Where, W_i = initial weight of sample (before digesting)

W_p = post weight of sample (after digesting)

11. Related works of silk degradation

11.1 Arai et. al., 2004

According to Arai et. al. study [27], the effects of silk fibroin biodegradation by various enzymes found in tissues where the ACL scaffold would be implanted were investigated. Collagenase Type F, α -chymotrypsin Type I-S, and protease Type XXI from *Streptomyces griseus* were selected for treating on fibroin fibers and films, all samples were incubated at 37 °C. The results of weight loss treated by each enzyme are shown in Table 2.6.

Table 2.6 Weight loss of silk fibroin [27]

Degradation time (days)	Weight loss (%)					
	collagenase		α -chymotrypsin		protease	
	a	b	a	b	a	b
1	2.6	3.8	6.0	9.0	18.2	35.0
3	4.1	5.5	9.2	11.8	27.4	45.5
10	7.4	8.9	13.0	14.9	35.7	55.6
17	9.4	10.7	14.7	16.5	45.5	64.3

Enzyme to substrate ratio: (a) 1:20; (b) 1:8

The results showed that the protease was more effective than α -chymotrypsin and collagenase in silk degradation, which exhibited in the decrease of sample weight and degree of polymerization. Silks treated by protease lost their weight more than 50% within 17 days, while silks treated by collagenase and α -chymotrypsin lost their weight just only 10.7% and 16.5% respectively (enzyme per substrate = 1:8). Furthermore, they found that each enzyme was specific to each peptide bond, which had an influence on silk digesting. The data is shown in Table 2.7.

Table 2.7 Specific peptide bonds of enzymatic digestion [27]

Enzymes	Specific bonding
collagenase	X – Gly – Pro
α -chymotrypsin	X – Y
Protease	non-specific

X = Tyr, Phe, Trp, Val, Ile, Leu

Y = any amino acids

From Table 2.7, collagenase breaks the bond between X and glycine connecting to proline. The α -chymotrypsin is specific to X – Y bond. While protease is non-specific enzyme, this is a reason why the weight loss of fibroin treated by protease is greater than collagenase and α -chymotrypsin.

11.2 Horan et. al., 2005

From the study of Horan et. al. [7], an in vitro model system of proteolytic degradation of silk-fibroin fibers was developed. The changes in degradation of fibroin fibers by incubating with protease Type XIV from *Streptomyces griseus* at 37 °C were examined. The results showed that the decrease in fibroin diameter, failure strength, cycles to failure, and mass indicated the degradation of fibroin fibers.

It was found that after 10 weeks of incubation, the diameter of silk fiber reduced more than 66% of the initial diameter. Weight loss of silk fiber was greater than 50% for 42 days of incubation. The ultimate tensile strength (UTS) decreased by 50% of initial strength after 21 days. Cycles to failure after incubated with enzyme were about 125,000 cycles (prior to incubate the cycles were more than 125,000).

The results of FT-IR analysis of silk fibroin showed that the spectral peak of Amide I (1625 cm^{-1}) did not change in terms of position with time of digestion, while the Amide II (1516 cm^{-1}) was slightly decreased in intensity and slightly shift with time, with a small shoulder appearing at 1528 and at 1535 cm^{-1} (Figure 2.20).

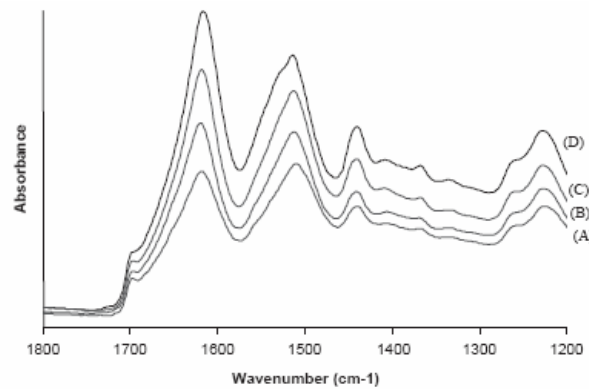


Figure 2.20 FT-IR spectra of silk fibroin incubated in 1.0 mg/ml protease for (A) 1 day, (B) 21 days, (C) 42 days or (D) 70 days [7]

The FT-IR data suggested that the structure of crystalline structure did not change (unchanged position of Amide I), with perhaps some loss of crystalline material (decreased Amide I) due to hydrolysis while digesting. Normally, the enzyme digested directly on amorphous structure, this caused the changes in Amide II in its intensity and position [7].

Gel electrophoresis indicated a decreasing amount of the light-chain silk fibroin at 25 kDa and a shifting to a lower molecular weight range of the heavy chain with increasing incubation time in protease, indicating that the degradation of both the light and heavy chains was occurred (Figure 2.21).

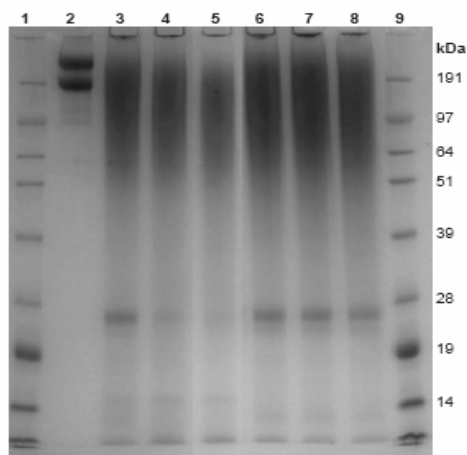


Figure 2.21 Gel electrophoresis of silk fibroin (Coomassie Blue staining): molecular weight marker (lanes 1 and 9), reduced laminin (lane 2), silk incubated in 1.0 mg/ml protease for 1 day (lane 3), 21 days (lane 4), 70 days (lane 5), or in PBS for 1 day (lane 6), 21 days (lane 7), and 70 days (lane 8) [7]

Furthermore, the SEM examination found that there was an increasing fragmentation of protease-digested silk with increasing incubation time (Figure 2.22). Silk's diameter decreased exponentially with time in protease.

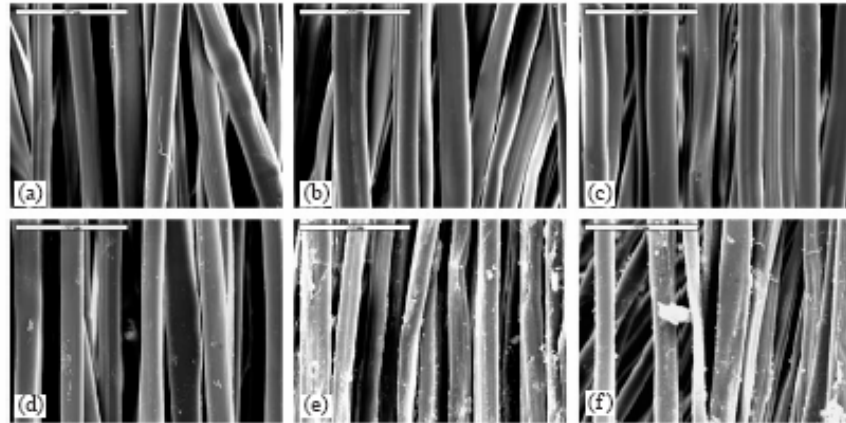


Figure 2.22 SEM images of silk fibers incubated in PBS for 1 day (a), 21 days (b), 42 days (c), and in 1.0 mg/ml protease solution for 1 day (d), 21 days (e) and 42 days (f) [7]

11.3 Li et. al., 2003

According to the study of Li et. al. [28], the in vitro enzymatic degradation behavior of porous silk fibroin sheets was investigated. Collagenase Type IA from *Clostridium histolyticum*, α -chymotrypsin, and protease Type XIV from *Streptomyces griseus* were used to digest the fibroin sheets.

The results showed that the protease was more effective to digest fibroin sheets than collagenase and α -chymotrypsin respectively. Throughout the degradation by protease XIV (Table 2.8), the amounts of Asp, Ser, Glu, Ala and Val in the degradation products increased with increasing times. These amino acids were released from the fibroin sheet and became degradation products. These showed that the protease XIV degraded not only dissolved silk fibroin, it also directly degraded the fibroin sheet into peptides and amino acids. Moreover, the percentage of free amino acids accounted for 67.6% of the total amount of the amino acids which composed of the degradation products on day 1, 57.3% on day 9, and 50.0% on day 15.

Table 2.8 Amino acid composition (g/100 g) of degradation products of porous silk fibroin sheets exposed to protease XIV [28]

Amino acids	Degradation solution		
	Day 1	Day 9	Day 15
Lys	1.85	1.19	2.11
His	1.51	ND	ND
Arg	3.36	2.25	1.05
Asp	ND	0.24	1.05
Thr	2.52	1.42	2.11
Ser	1.68	2.49	3.16
Glu	ND	0.71	2.11
Pro	ND	ND	ND
Gly	2.69	11.61	14.04
Ala	6.74	26.21	30.86
Cys	22.18	18.74	17.19
Val	1.34	1.41	2.11
Met	12.77	10.56	12.63
Ile	5.04	1.19	1.40
Leu	6.39	3.08	3.86
Try	24.54	15.66	2.11
Phe	7.39	3.20	4.21

ND: not determined

From the studies of Arai et. al., Horan et. al., and Li et. al., it may be concluded that the protease enzyme plays an important role in digesting the silk fibroin than the others.

11.4 Sampaio et. al., 2005

From a study of Sampaio et. al. [23], the potential of using mushroom tyrosinase to graft the chitosan onto silk fibroin was investigated. FT-IR results showed that there was a shoulder gradually appeared at 1650 cm^{-1} of Amide I when

treated with higher concentration of mushroom tyrosinase. This band indicated to the increasing of o-quinone residues, which were tyrosine's oxidation products. Whereas, a shoulder at 1262 cm^{-1} of Amide III was gradually disappeared indicating to the transformation of β -sheet to random coil conformations (Figure 2.23).

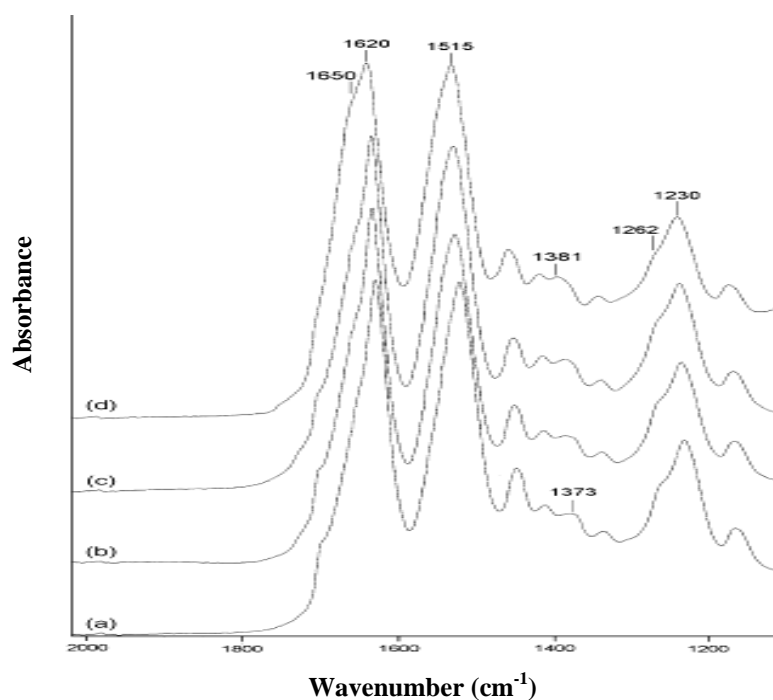


Figure 2.23 FT-IR spectra of silk fibroin without mushroom tyrosinase (a), with 0.38 U/mg mushroom tyrosinase (b), with 0.72 U/mg mushroom tyrosinase (c), and with 3.3 U/mg mushroom tyrosinase (d) [23]

11.5 Tsuboi et. al., 2001

From a report of Tsuboi et. al. [29], they showed how to transform the secondary structure of silk fibroin by laser light. They found that a 266 nm laser light was capable to transform the secondary structure of random coil to β -sheet structure. This was examined by the appearance of the shoulders at 1695 cm^{-1} in Amide I and 1260 cm^{-1} in Amide III (Figure 2.24). However, the Amide II band was difficult to distinguish the secondary structure because the spectral shape was broad due to these structures (1540 cm^{-1} for the random-coil structure and 1520 cm^{-1} for the β -sheet structure). Whereas, the transformation from β -sheet to random coil structures could be done by using a 248 nm laser light, which had no spectrum data.

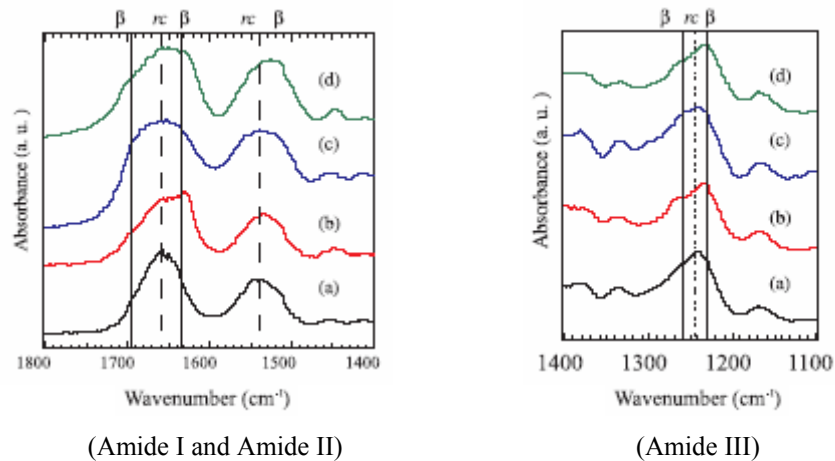


Figure 2.24 FT-IR spectra changes of silk fibroin: A spectrum of neat fibroin film with random coil structure (a), after a thermal treatment at 470 K (b), after 266 nm irradiation (c), and commercially supplied fibroin whose secondary structure was of mixed type of β -sheet and random coil structures [29]

11.6 Shoa et. al., 2005

According to Shoa et. al. [25], the degradation of silk fibroin exposed to UV/ozone irradiation for 40 minutes by FT-IR was investigated (Figure 2.25). The FT-IR results showed a decreasing of crystallinity degree of irradiated silk fibroin (from 47.7% to 41.8%), which could be determined from the doublets of Amid III (1230 and 1263 cm^{-1}). The signal at 1263 cm^{-1} was associated with β -pleated-sheet conformation, while the signal at 1230 cm^{-1} was associated with α -helix or random coil conformation. By comparing the areas of both 1263 and 1230 cm^{-1} , we could qualitatively and quantitatively analyze the crystallinity degree of silk fibroin following equation 2.6:

$$\text{Crystallinity degree (\%)} = \frac{A_{1263}}{(A_{1230} + A_{1263})} \times 100 \quad (2.6)$$

The intensive UV/ozone irradiation caused a considerable decrease in the silk crystallinity degree, because of a molecular rearrangement accompanied by peptide fission.

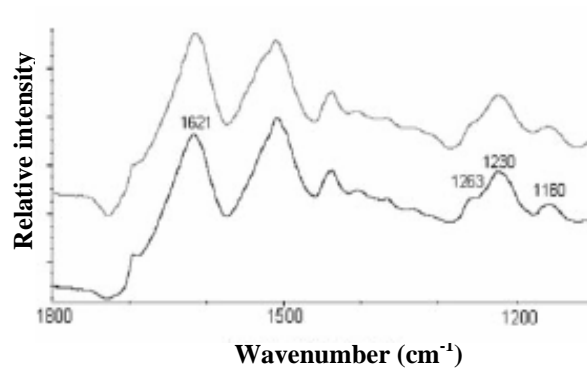


Figure 2.25 FT-IR spectra of non-irradiated silk (lower curve), and UV/ozone irradiated silk for 40 min (upper curve) [25]

11.7 Pewlong et. al., JAERI Conference 2000-2003

According to Pewlong et. al. [30], the degradation of silk fibroin irradiated with an electron beam accelerator at various dosages ranging from 500 to 2500 kGy in both oxygen atmosphere and vacuum was examined. The results showed that the tensile strength of irradiated fibroin fiber decreased with increasing irradiated dose. The tensile strength of fibroin fiber irradiated up to 1500 kGy in oxygen decreased to 13% of that for unirradiated fibroin fiber, whereas 25% for the same dose in vacuum. The tensile strength of fibroin fiber irradiated more than 2000 kGy in oxygen could not be measured due to the severely degradation (Figure 2.26).

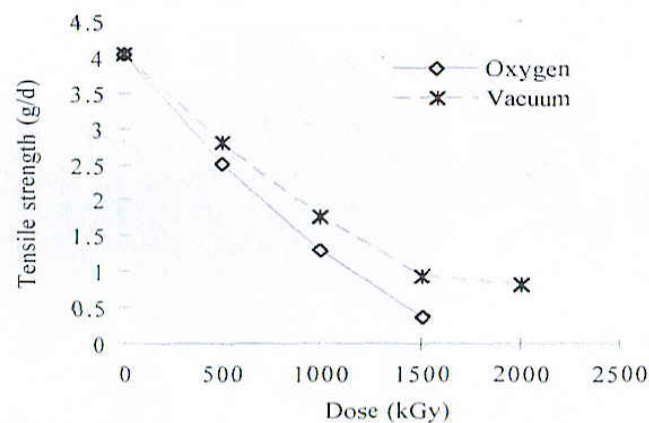


Figure 2.26 Tensile strength of irradiated silk fibroin fibers [30]

Furthermore, the irradiated fibroin fibers became water-soluble fibers compared to the unirradiated fibers, which were originally insoluble. The ability of

water dissolving increased with the increasing irradiated dose. The dissolved fractions of fibroin fibers irradiated at 2500 kGy were approximately 43% for oxygen condition and about 30 % for vacuum (Figure 2.27).

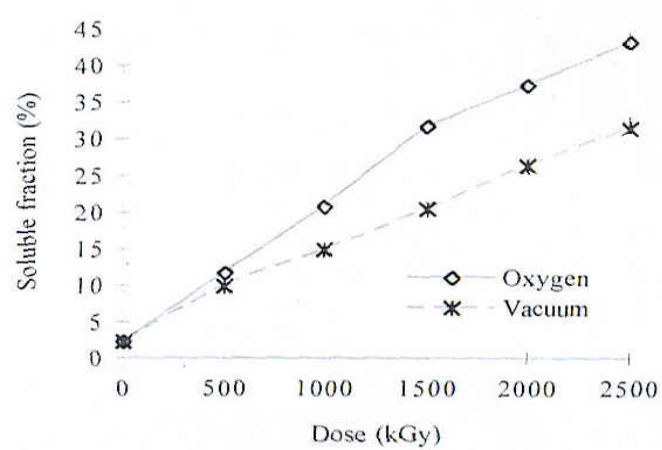


Figure 2.27 Effect of radiation on solubility of silk fibroin fibers in distilled water [30]

CHAPTER III

MATERIALS AND METHODS

1. Materials

- 1.1 Silk fibers and cocoons of *Bombyx mori* var. *Nangnoi Sisaket-1*
(obtained from The Queen Sirikit Institute of Sericulture, Thailand)
- 1.2 Fibroblast cells (obtained from Department of Pathobiology, Faculty of Science, Mahidol University)
- 1.3 Whole blood (obtained from Department of Pathobiology, Faculty of Science, Mahidol University)
- 1.4 Calcium chloride dihydrate, $\text{CaCl}_2 \cdot 2\text{H}_2\text{O}$ (MERCK, Germany)
- 1.5 Ethanol, $\text{C}_2\text{H}_5\text{OH}$ (MERCK, Germany)
- 1.6 Protease type XIV from *Streptomyces griseus* (Sigma, USA)
- 1.7 Phosphate buffered saline (PBS), pH 7.4
- 1.8 Cell culture media (5% fetal calf serum in RPMI media)
- 1.9 Heparin
- 1.10 Glutaraldehyde 0.5%
- 1.11 Potassium bromide, KBr (Sigma, USA)
- 1.12 Broad range marker (BIO-RAD)
- 1.13 Geimsa dye
- 1.14 Commassie Blue dye
- 1.15 Regenerated cellulose tubular membrane T4, Nominal MWCO; 12,000-14,000 (Cellusep)
- 1.16 35 mm Polystyrene Petri dish (Corning, USA)
- 1.17 Hydraulic press
- 1.18 Incubator
- 1.19 CO_2 incubator (SHEL LAB)
- 1.20 Centrifuge (Universal 32R, Hettich ZENTRIFUGEN, Germany)

- 1.21 Inverted light microscope (CKX 41, Olympus)
- 1.22 Vertical electrophoresis units (BIO-RAD)
- 1.23 Gamma irradiator (Gammacell 220 Excel, MDS Nordian)
- 1.24 FT-IR spectrometer (Spectrum GX, PERKIN ELMER)
- 1.25 UV/VIS spectrometer (Lambda 35, PERKIN ELMER)
- 1.26 SEM (XL30 & EDAX, Philips)

2. Methods

2.1 Silk degumming

Raw silk fibers and cocoons of *Bombyx mori* var. *Nangnoi Sisaket-1* were subjected to remove sericin by degumming process following Meesilpa et. al. [31] method.

2.2 Fibroin film preparation

A 0.5 g of degummed cocoons was boiled in $\text{CaCl}_2 \cdot 2\text{H}_2\text{O}$: $\text{C}_2\text{H}_5\text{OH}$: H_2O , in a ratio of 1: 2: 8 by mole. Fibroin solution was transferred into cellulose tubular membrane, and then dialyzed in distilled water for 3 days. The fibroin solution contained in cellulose membrane was transferred into a Petri dish, and drying at room temperature. After drying, the film could be peeled off from the dish.

2.3 Gamma irradiation

Silk samples were irradiated by a gamma irradiator. The gamma irradiation process was supported by the Office of Atoms for Peace, Thailand.

2.4 In vitro biodegradation test

Degummed silk fibers were irradiated with different doses (0, 100, 500 and 1000 kGy). 80 mg of each was put into closed tubes containing 2 ml of 1 mg/ml protease solution. The negative control of biodegradation study was prepared by immersing the degummed silk fibers in PBS at pH 7.4 without enzyme. All sample tubes were incubated at 37 °C for 28 days. Degradation analysis was done every 7

days by collecting 0.5 ml of degradation solution for analyzing spectrophotometry and gel electrophoresis. After collecting the 0.5 ml solution from each sample, the 0.5 ml of 1 mg/ml protease was refilled into the sample tube to preserve the solution level and enzyme activity. The enzyme treated silk fibers were collected and dried at 80 °C for 3 hr. The weight loss measurement, SEM analysis (done only 28 days), and FT-IR analysis were performed to evaluate the biodegradation rate of each sample.

2.5 Test of cell growth

Irradiated fibroin fibers (0, 100, 500 and 1000 kGy) sterilized by gamma radiation were put into Petri dishes. Prepared fibroblast cells were dropped on the fibroin fibers. The cell culture media was added into the culture dishes, and incubated at 37 °C with 5% CO₂. The culture media was changed every 3 days. Cell attachment and growth were observed at days 3 and 7 of culturing by inverted light microscope.

2.6 In vitro white blood cell activation test

The 5 ml of whole blood from a donor was mixed with 5 µl of heparin as anticoagulant. This mixture was then centrifuged twice in RPMI media (using speed 2000 rpm, 10 min) to remove the heparin. The centrifuged blood was suspension in 5 ml of 5% fetal calf serum in RPMI media, then 1:2 dilutions with RPMI media was prepared. The diluted blood was transferred into sterilized fibroin films and fibroblast grown on fibroin films (the films were coated on Petri dishes). All samples were incubated at 37 °C with 5% CO₂ for 15, 30, 45, 60, 120 and 180 min. After incubations, the films were washed with 37 °C PBS, and then fixed the cells twice with 0.5% glutaraldehyde for 2 min. The fixed films were washed again with distilled water before Geimsa staining. White blood cells on fibroin film could be observed by inverted light microscope. Amounts of white blood cells attaching to the fibroin film could be counted with 19 mm² cell counter grid via a light microscope.

2.7 Fourier transform infrared spectroscopy

Dry silk samples were ground in a mortar to be powders. A 0.2 mg silk powder was mixed with 80 mg of KBr, and ground into fine powder. The mixture was compressed by a hydraulic press forming a sample-KBr tablet, which was subjected to

analyze by FT-IR spectrometer. The wavenumbers used in this study was varied from 2000 to 700 cm^{-1} .

2.8 Spectrophotometry

A 0.5 ml sample solution was transferred into a quartz crystal cuvette preparing to analyze. For analysis, blank and sample cuvettes were inserted together for detecting in a spectrometer. A background of measurement would be automatically deleted from the sample. Protease-PBS mixture was used as a blank of protease-associated degradation products, while the PBS was used as a blank of negative control sets. A wavelength applied in this study was 280 nm.

2.9 Gel electrophoresis

A 0.5 ml of degradation solutions from biodegradation test were mixed with 10 μl of protease inhibitor before stored at $-70\text{ }^{\circ}\text{C}$ (no protease inhibitor for negative control samples). All samples were run on 12% resolving gel under electrical current 120 volts. Broad range marker was run as a molecular weight marker (203-7.6 kDa) on all gels. Gels were stained by colloidal Commassie Blue staining.

2.10 Scanning electron microscopy

Dry fibroin fibers were affixed by carbon tape to the SEM sample holders. The fibers were coated with gold for 45 sec and examined the morphology of sample by scanning electron microscope.

CHAPTER IV

RESULTS

1. Effect of radiation on silk fibroin

There were physical and mechanical changes of silk fibroin fibers after gamma radiation. Physical changes could be observed in the color, scent and morphology. The color was gradually dark and the scent was strong with increasing irradiation dose (Figure 4.1). The morphology examination by SEM showed the increasing of erosion and cleft when the higher irradiation dose was applied (Figure 4.2). Also, the mechanical property, such as tensile strength was decreased at the high-irradiation intensity. Thus, they were torn easily.

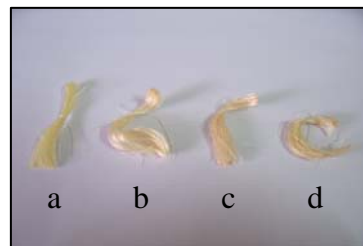


Figure 4.1 Appearance of silk fibroin fibers after gamma irradiation: unirradiated fibers (a), 100 kGy (b), 500 kGy (c), and 1000 kGy (d)

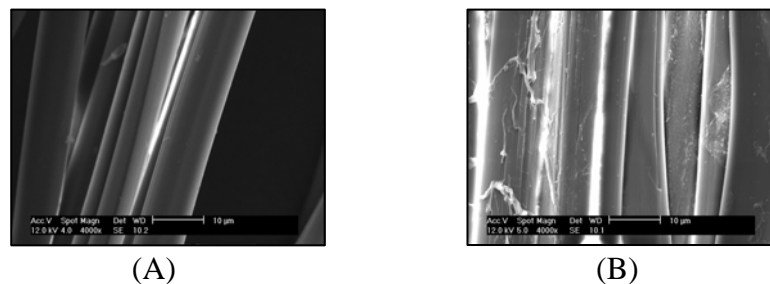


Figure 4.2 SEM images of silk morphology after gamma irradiation: unirradiated fibers (A), and 600 kGy (B)

The FT-IR analysis of irradiated silk fibroin was shown in Figure 4.3. The areas of Amide I, Amide II, and Amide III were increased with increasing irradiation dose, while the area ratio of Amide I and Amide II trended to be stable (Table 4.1). The 1263 cm^{-1} peak was gradually disappeared with the increasing dose. The crystallinity degree of silk fibroin calculated as the equation 2.2 found that it decreased when the higher irradiation intensity was applied. The crystallinity degree decreased from 45.3% of unirradiated fibroin to 28.5% of 3000 kGy irradiated fibroin as shown in Figure 4.4.

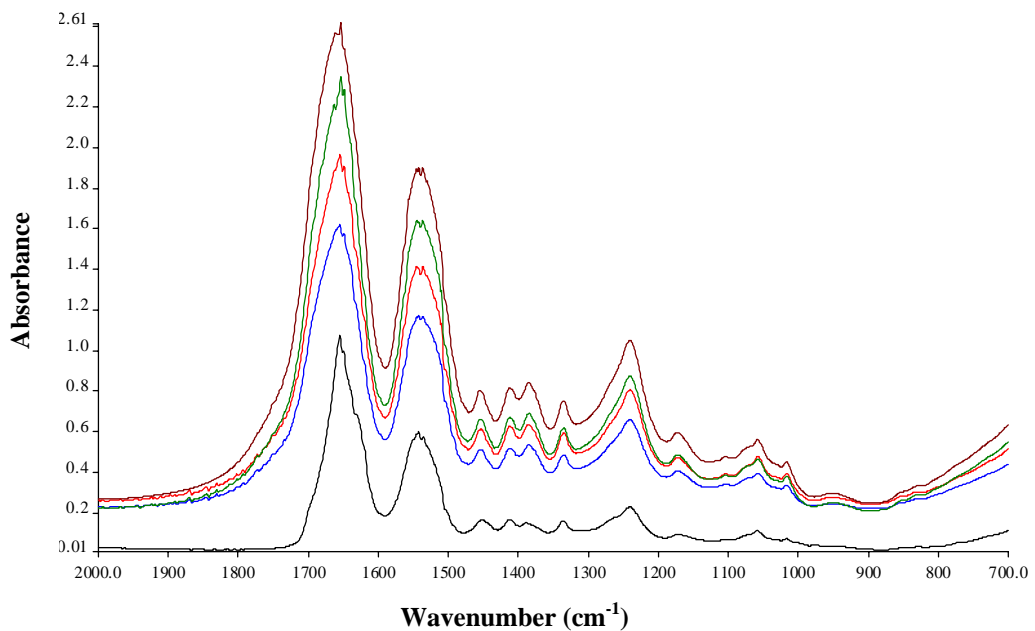


Figure 4.3 FT-IR spectra of irradiated silk fibroin: 0 kGy (black), 1000 kGy (blue), 1500 kGy (red), 2000 kGy (green) and 3000 kGy (brown)

Table 4.1 Peak areas of Amide I, Amide II, Amide III, and Amide I per Amide II of silk fibroin at different irradiation doses

Dose (kGy)	Amide I (A.cm^{-1})	Amide II (A.cm^{-1})	Amide III (A.cm^{-1})	Amide I / Amide II
0	48.6466	22.6727	6.2639	2.1456
1000	90.9404	39.4537	13.6458	2.3050
1500	107.4109	48.9919	17.3215	2.1924
2000	132.3398	59.6200	20.6564	2.2197
3000	153.8475	65.5894	23.6421	2.3456

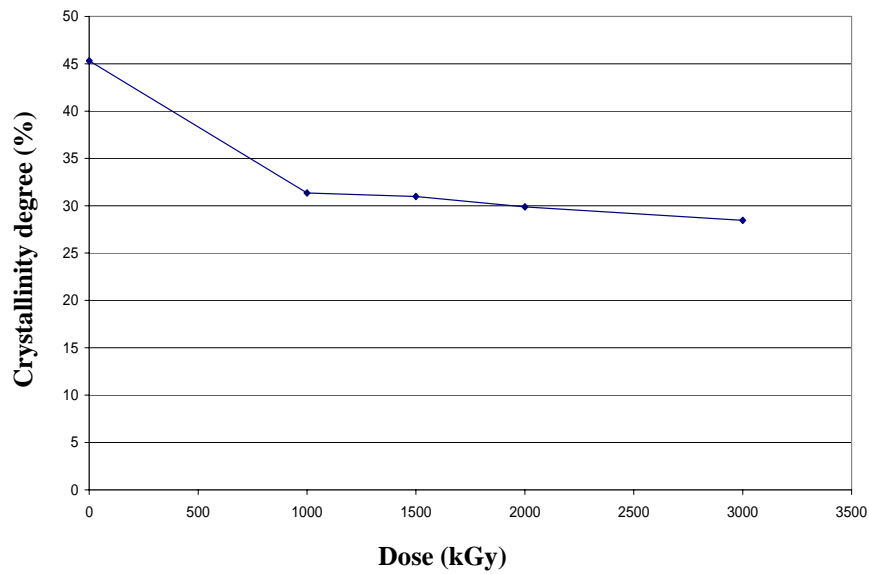


Figure 4.4 Crystallinity degree of silk fibroin at different irradiation doses

Effect of gamma radiation on water solubility of silk fibroin films found that the fibroin film did not dissolve in water when using the intensity less than 400 kGy, whereas, the fibroin films could be dissolved in water when using the irradiation intensity from 400 kGy to 1000 kGy. The time required for complete dissolution was decreased linearly as the radiation intensity increased until 1000 kGy. The capacity of dissolving trended to be stable at intensity over 1000 kGy, which corresponded to the dissolution of 5 min (Figure 4.5).

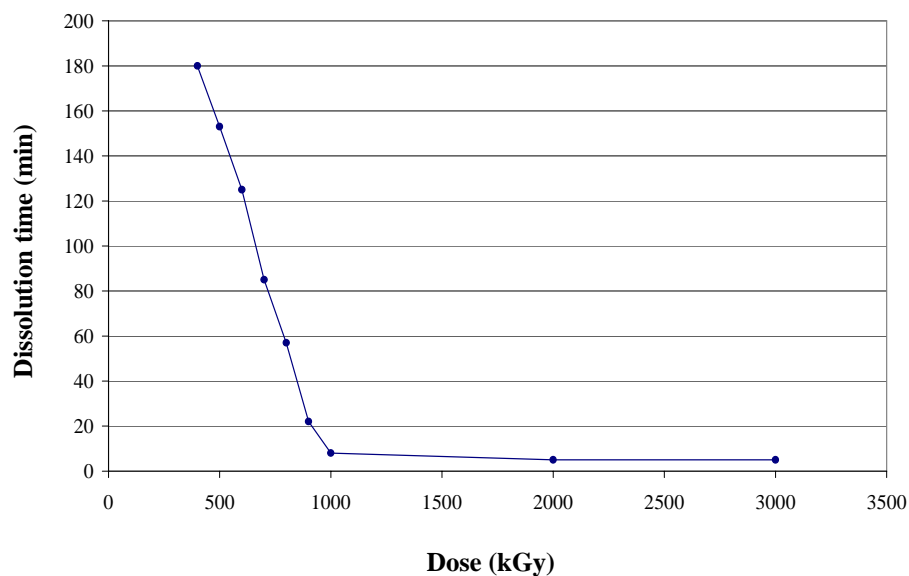


Figure 4.5 Water dissolution of silk fibroin film at different irradiation doses

2. In vitro biodegradation test

In vitro degradation was observed in all silk samples incubated in 1 mg/ml protease. The first notice observed on silk degradation test was the silk fragment precipitate in the solution. The higher irradiation dose applied, the larger amount of silk sediments was found. This also correlated to the color of the sample, which a darker color was observed when the silk sample was exposed to a higher irradiation dose (Figure 4.6).

The weight loss due to the degradation of silk fibroin showed that the weight loss of silk fibers was proportional to intensity of radiation and degradation time. More than 50% of weight loss occurred within 14 days found in 1000 kGy irradiated silk fibroin. There was no change in mass of unirradiated sample in negative control condition. The results of weight loss measurement were shown in Table 4.2.

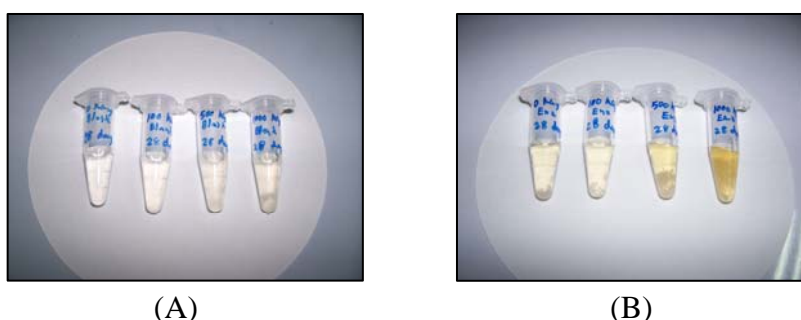


Figure 4.6 Degradation products of irradiated silk fibroin (0, 100, 500 and 1000 kGy from left to right, respectively) for 28 days: (A) is control, (B) is in 1 mg/ml protease.

Table 4.2 Weight loss percentages of irradiated silk fibroin incubated in 1 mg/ml protease in 7, 14, 21 and 28 days.

Dose (kGy)	Weight loss (%)							
	7 days		14 days		21 days		28 days	
	C	E	C	E	C	E	C	E
0	0	1.22	0	2.44	0	8.54	0	14.63
100	0	2.44	1.22	4.88	6.10	15.85	14.63	25.61
500	9.88	20.99	13.58	25.93	20.98	34.86	26.83	47.04
1000	18.29	32.93	25.61	52.44	40.24	67.07	47.56	78.05

Control condition (C), Enzyme condition (E)

Morphology of silk fibroin digested by protease was observed via SEM (Figure 4.7). The results showed that at the higher radiation intensity, the clefts on the silk fibroin were increased in both sample with and without protease.

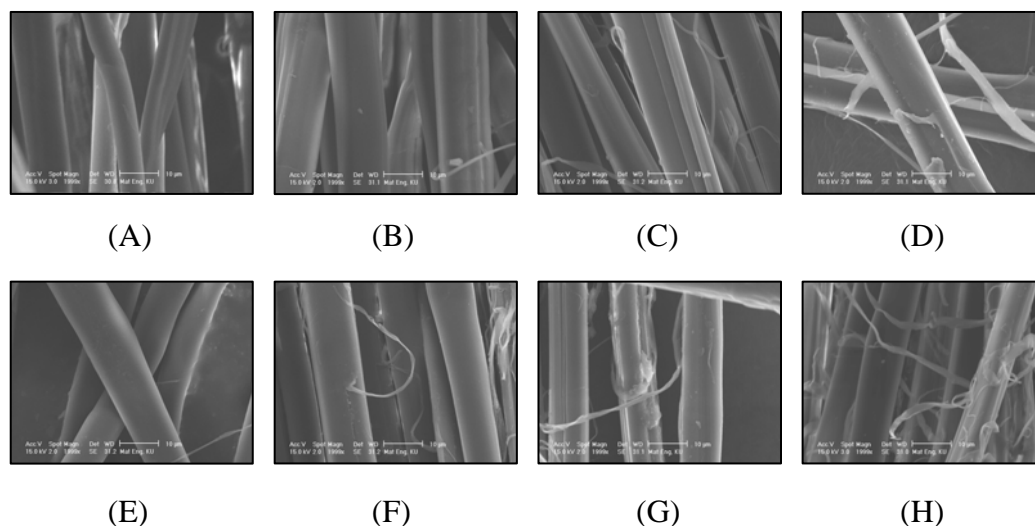


Figure 4.7 SEM images of irradiated silk fibroin incubated in PBS (control): 0 kGy (A), 100 kGy (B), 500 kGy (C) and 1000 kGy (D), and in 1 mg/ml protease for 28 days: 0 kGy (E), 100 kGy (F), 500 kGy (G) and 1000 kGy (H)

FT-IR spectra of irradiated silk fibroin treated by PBS (control) and 1 mg/ml protease for 28 days are showed in Figures 4.8 and 4.9 respectively. The results showed that the areas of Amide I, Amide II, Amide III, and Amide I per Amide II were increased with increasing irradiation dose in both control and enzymatic conditions (Tables 4.3 and 4.4). There were two distinguishable peaks (1695 and 1650 cm^{-1}) occurred in the Amide I band. The 1650 cm^{-1} peak was gradually increased and sharp at a higher irradiation dose in both control and enzymatic conditions.

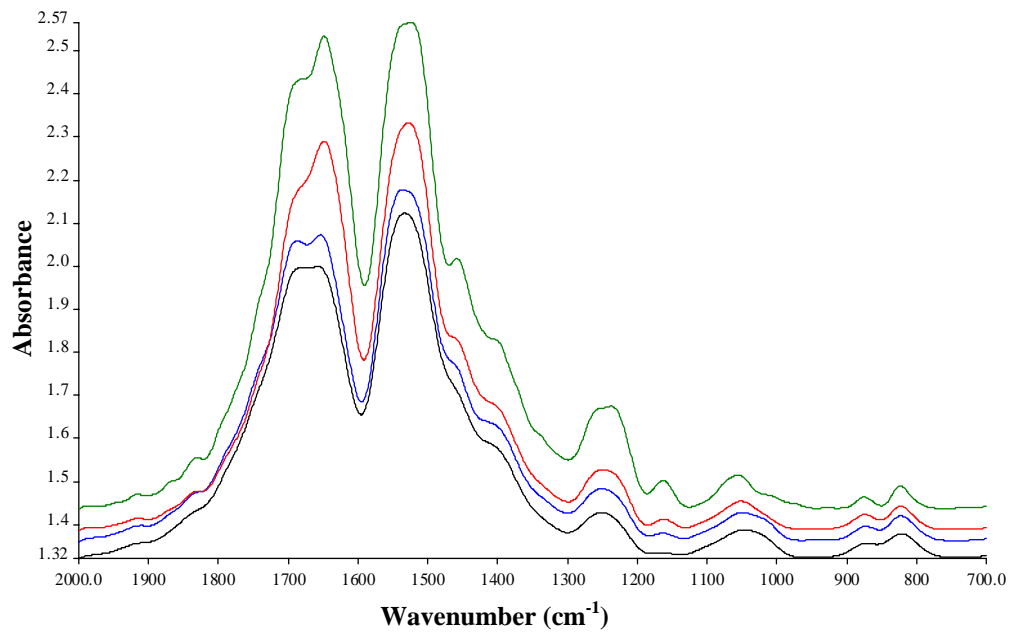


Figure 4.8 FT-IR spectra of irradiated silk fibroin incubated in PBS (control) for 28 days: 0 kGy (black), 100 kGy (blue), 500 kGy (red) and 1000 kGy (green)

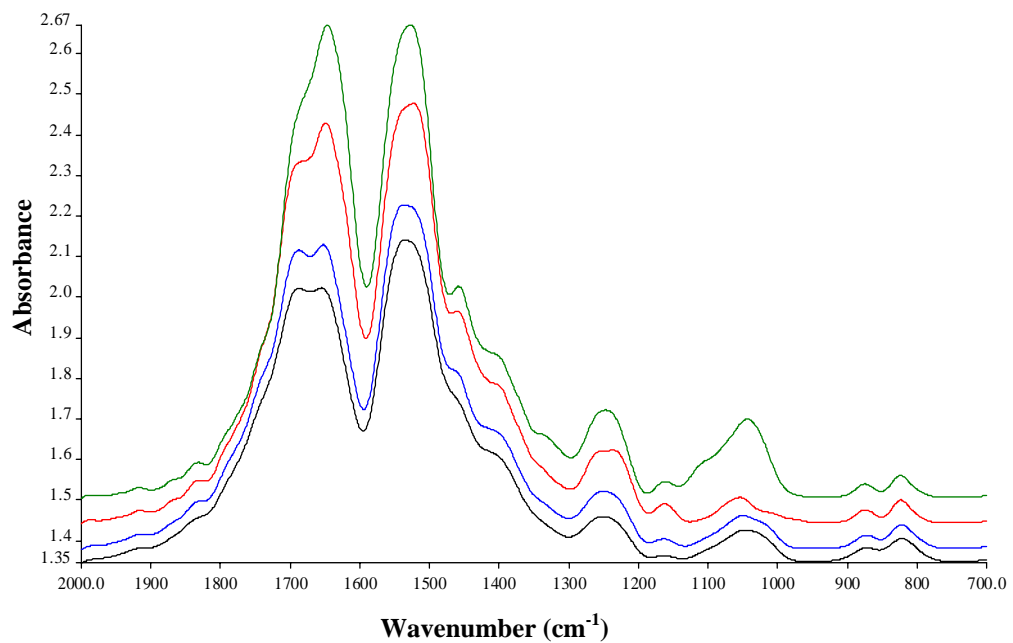


Figure 4.9 FT-IR spectra of irradiated silk fibroin incubated in 1 mg/ml protease for 28 days: 0 kGy (black), 100 kGy (blue), 500 kGy (red) and 1000 kGy (green)

Table 4.3 Peak areas of Amide I, Amide II, Amide III, and Amide I per Amide II of irradiated silk fibroin treated by PBS for 28 days

Dose (kGy)	Amide I (A.cm⁻¹)	Amide II (A.cm⁻¹)	Amide III (A.cm⁻¹)	Amide I / Amide II
0	49.3874	40.7084	3.2437	1.2132
100	53.8015	42.7485	4.1442	1.2586
500	61.9215	46.6972	6.2200	1.3260
1000	77.0876	53.2378	10.3756	1.4480

Table 4.4 Peak areas of Amide I, Amide II, Amide III, and Amide I per Amide II of irradiated silk fibroin treated by 1 mg/ml protease for 28 days

Dose (kGy)	Amide I (A.cm⁻¹)	Amide II (A.cm⁻¹)	Amide III (A.cm⁻¹)	Amide I / Amide II
0	50.3394	41.0786	3.6019	1.2254
100	56.2496	43.9052	5.7867	1.2812
500	69.5262	51.2330	8.1157	1.3571
1000	74.0666	51.9476	9.1959	1.4258

Optical density (O.D.) at wavelength 280 nm was measured in all degradation products by spectrophotometer. The results showed that the increasing of O.D. was proportional to the radiation dose and incubation time (Table 4.5).

Table 4.5 Measurement of optical density at 280 nm of degradation products incubated in PBS (control) and 1 mg/ml protease at different times.

Dose (kGy)	Optical density (O.D.) at 280 nm							
	7 days		14 days		21 days		28 days	
	C	E	C	E	C	E	C	E
0	0.35188	1.46234	0.35135	1.53153	0.35292	1.58452	0.35116	1.62021
100	0.98139	1.52444	1.35512	1.58914	1.55062	1.64932	1.59144	1.70013
500	1.22365	1.55586	1.50046	1.61007	1.59483	1.69989	1.65928	1.81371
1000	1.36463	1.57929	1.53392	1.68806	1.65515	1.76914	1.67426	1.88314

Control condition (C), Enzyme condition (E)

Additionally, an activity of protease was observed by spectrophotometer at the wavelength of 800-200 nm. The results showed that there was a sharp peak occurred at 280 nm on the sample incubated for 7 days (Figure 4.10).

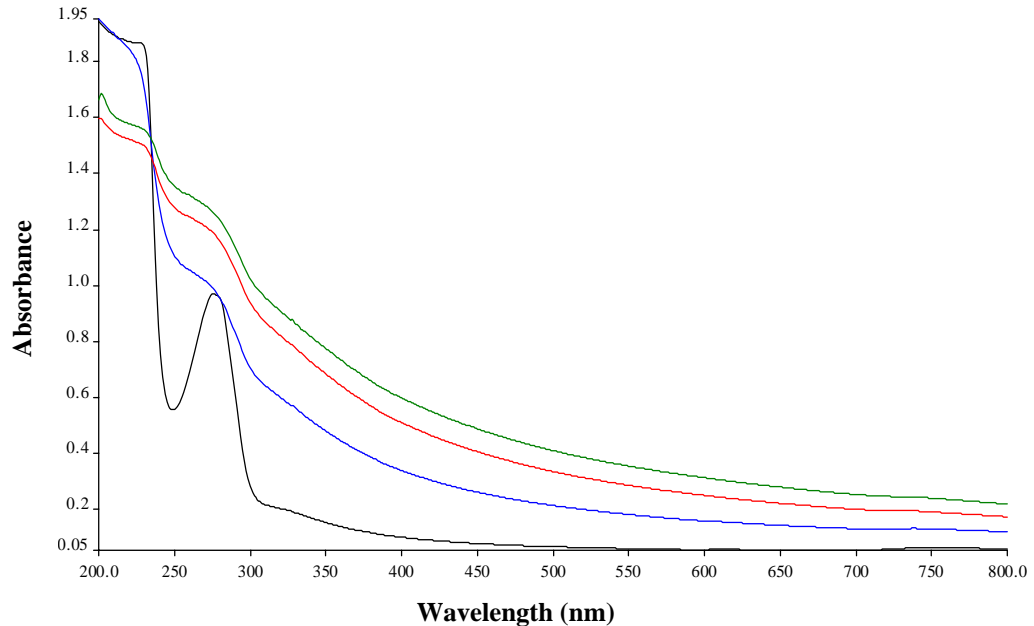


Figure 4.10 Spectrophotometry analysis of 1 mg/ml protease incubated for 7 days (black), 14 days (blue), 21 days (red) and 28 days (green)

Gel electrophoresis results showed two low-molecular weight proteins existing in enzymatic degradation products (lanes 7 to 10), i.e. 37 and 33 kDa (Figure 4.11). Whereas, there was no proteins found in control condition (lanes 3 to 6).

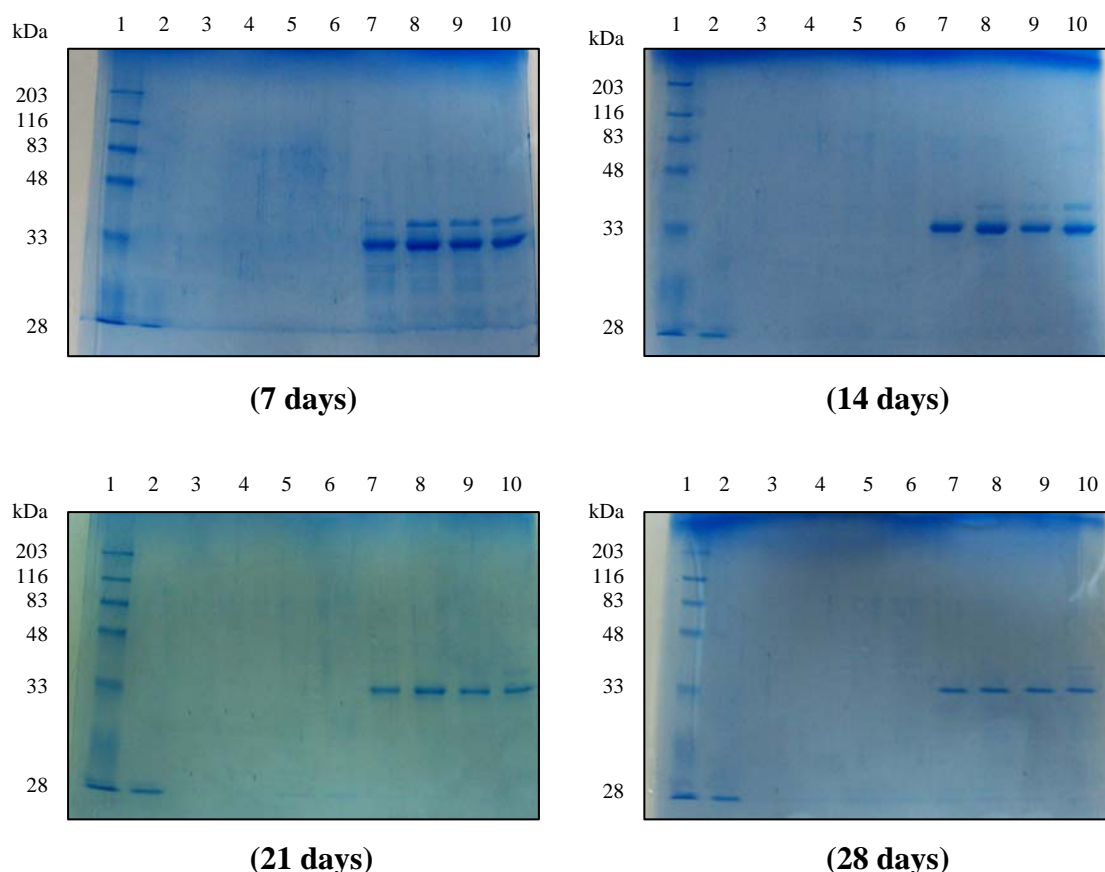


Figure 4.11 Gel electrophoresis of degradation products: molecular weight marker (lane 1), 1 mg/ml protease (lane 2), control conditions of unirradiated sample (lane 3), 100 kGy (lane 4), 500 kGy (lane 5), 1000 kGy (lane 6), enzymatic conditions of unirradiated sample (lane 7), 100 kGy (lane 8), 500 kGy (lane 9) and 1000 kGy (lane 10)

3. Effect of irradiation on cell growth

A cell growth on irradiated silk fibroin was observed by seeding fibroblast cells onto silk fibroin fibers irradiated with different doses (0, 100, 500 and 1000 kGy). Cell growth observation was done within 3 and 7 days via an inverted light microscope (Figures 4.12 and 4.13).

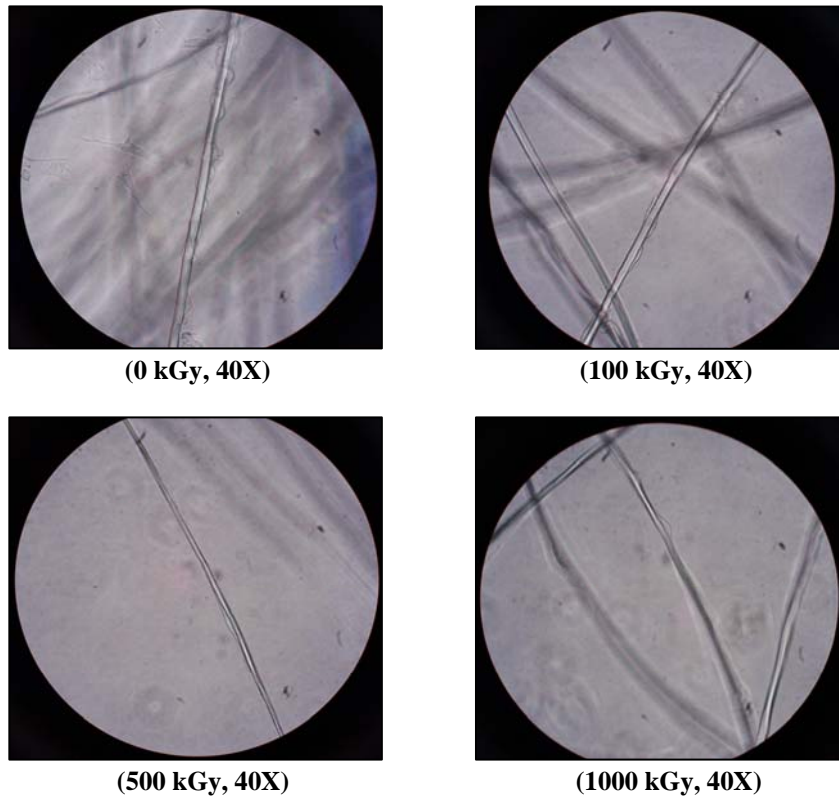


Figure 4.12 Fibroblasts grow on irradiated fibroin fibers (3 days of culturing).

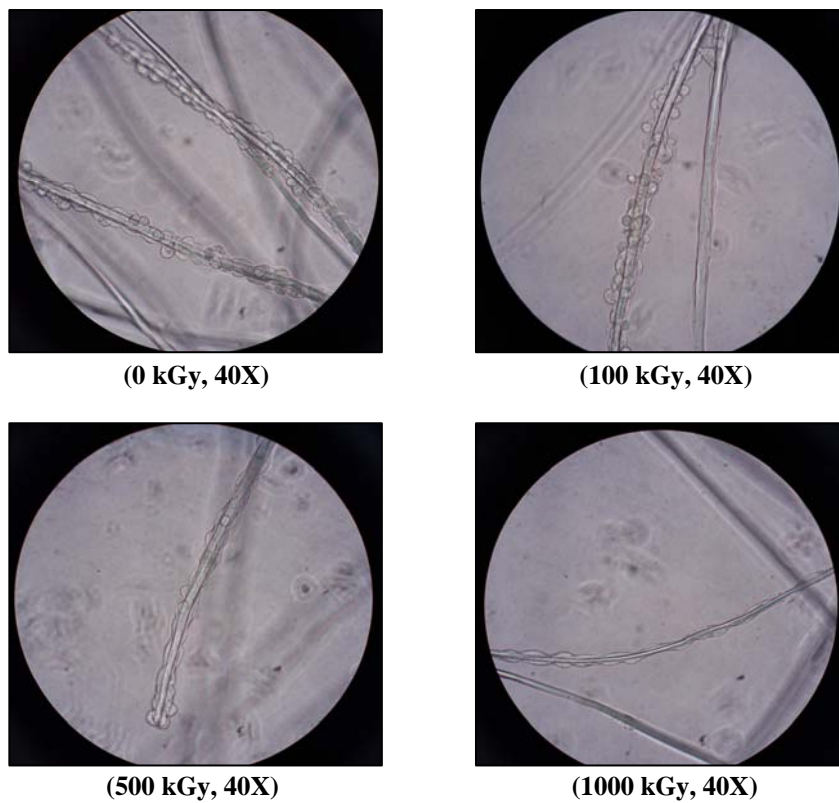


Figure 4.13 Fibroblasts grow on irradiated fibroin fibers (7 days of culturing).

The numbers of cell growth on the fibroin fibers irradiated with different intensities were shown in Table 4.6. The cell count was done via a 19 mm² cell counter grid. Data of cell count was average from 50 fields of observation via 40X magnification of inverted light microscope.

Table 4.6 Amounts of cell growth on irradiated silk fibroin fibers

Dose (kGy)	Cell count (cells / 19 mm ²)	
	3 days	7 days
0	10.5	33.7
100	5.3	25.4
500	2.2	12.1
1000	0.3	6.2

4. In vitro white blood cell activation test

This additional study of white blood cell activation was carried out in order to check the biocompatibility of degummed silks by in vitro testing with human white blood cells. The test was done on fibroin films and fibroblast grown on fibroin films by varying the incubation times (15, 30, 45, 60, 120 and 180 min). The testing results of fibroin films and fibroblast grown on fibroin films were shown in Figures 4.14 and 4.15 respectively.

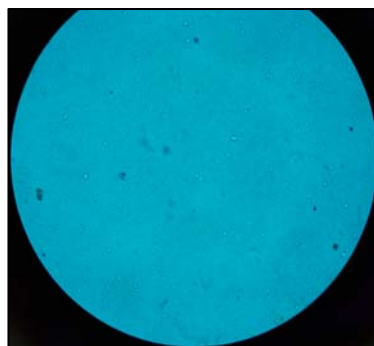
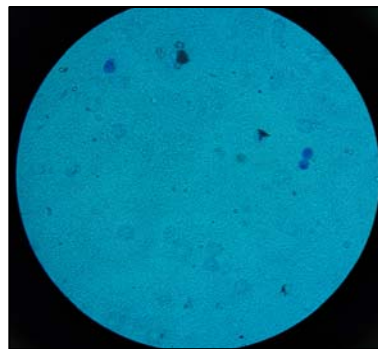
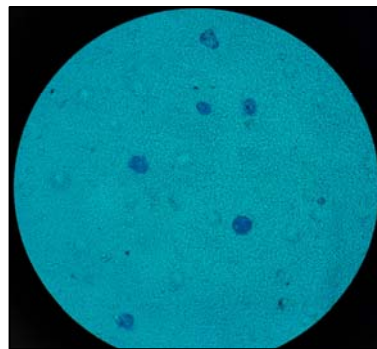


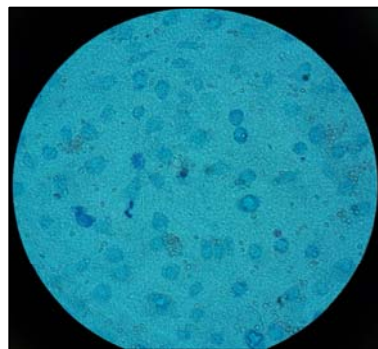
Figure 4.14 Blank fibroin film with non-activation of white blood cells (60 min of incubation time, 40X)



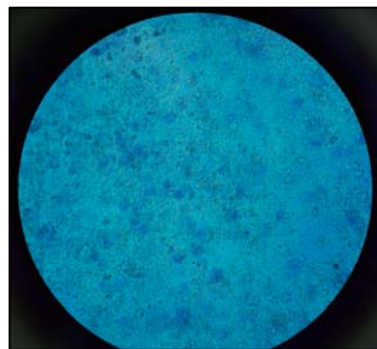
(15 min, 40X)



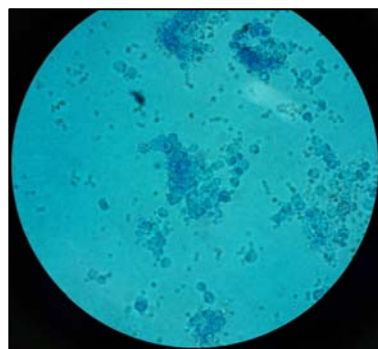
(30 min, 40X)



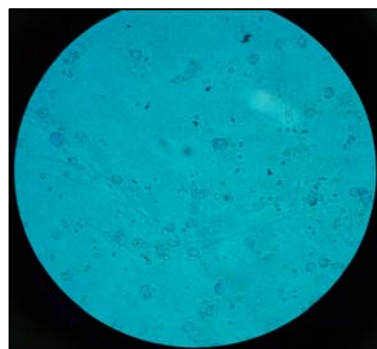
(45 min, 40X)



(60 min, 40X)



(120 min, 40X)



(180 min, 40X)

Figure 4.15 White blood cell activation to the fibroin film growing with fibroblasts incubated in different times (15, 30, 45, 60, 120 and 180 min). Blue-color cells were neutrophils and the transparent cells were monocytes.

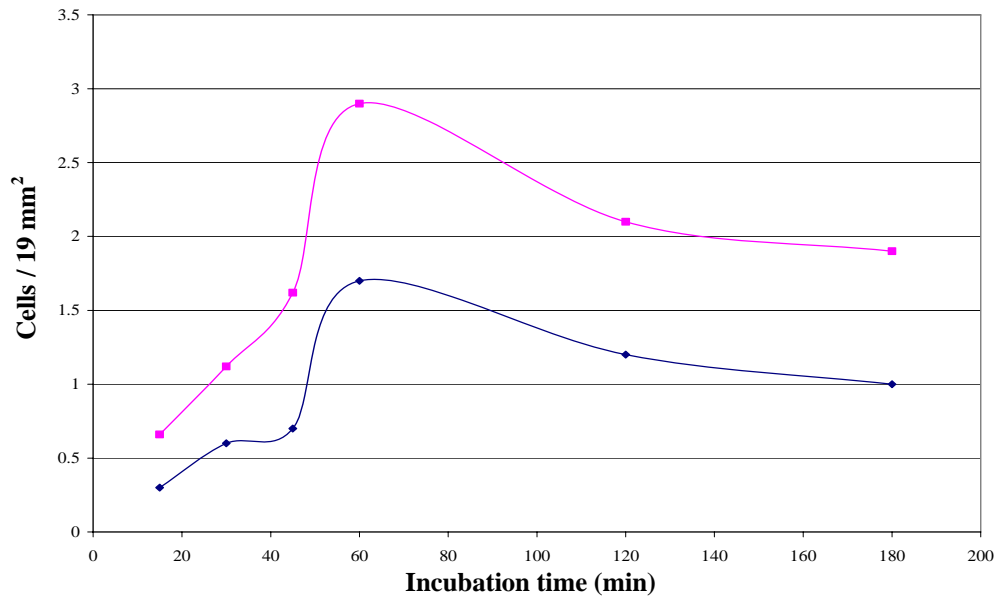


Figure 4.16 White blood cell count on activated fibroin films (film + fibroblast) incubated in different times. Monocyte count (upper curve) and neutrophil count (lower curve)

Figure 4.16 showed a time period of white blood cells activation to the fibroin film growing with fibroblasts. There were two types of white blood cell found, monocyte and neutrophil.

CHAPTER V

DISCUSSION

Gamma radiation affected directly to the changes of physical and mechanical properties of silk fibroin. The radiation could change the structure of silk fibroin, which could be examined by FT-IR analysis. Increasing of Amide I, Amide II, and Amide III in Figure 4.3 indicated that the peptide bond (C-N) in polypeptides become weak. As mentioned earlier, the Amide I, Amide II, and Amide III spectra occurred from bonding vibrations. When the peptide bond became weakness, the bond could be trembled easily impelling the vibrational transfer to other bonds increased. Therefore, the Amide I, Amide II and Amide III vibrations were increased. These could be explained to silk degradation caused by radiation. Furthermore, the effect of radiation caused the reduction of crystallinity degree of silk fibroin due to the reduction of β -sheet structure (Figure 4.4). At the Amide III band, the 1263 cm^{-1} peak was gradually disappeared with increasing the irradiation doses. These showed the reduction of β -sheet conformation, which was converted to random coil conformation. The area ratio of Amide I and Amide II showed the correlation between the crystalline phase and amorphous phase in the silk fibroin. The stable Amide I per Amide II ratio of silk fibroin irradiated at different doses in Table 4.1 indicated that the gamma radiation did not affect to the portion change of crystalline and amorphous phases in silk fibroin even though the higher irradiation intensity was applied.

The results of secondary structure transformation (from β -sheet to random coil) of silk fibroin after gamma irradiation caused the silk fibroin films become water soluble. The hydrolysis occurred to the random coil structure was easier than the β -sheet structure, because the hydrogen bonding inside the random coil structure was occurred between the successive turns of the helix of itself, while the hydrogen bonding inside the β -sheet structure was formed between the antiparallel-polypeptide strands acting as reinforcement of the silk structure.

From the results of weight loss measurement in Table 4.2, the loss of silk mass was proportional to the radiation intensity and degradation time in both conditions of with and without protease. The degradation of the silk samples in enzymatic condition was occurred by hydrolysis and enzyme digestion, while the degradation in control condition was occurred by hydrolysis. The silk mass was lost more than 50% within 14 days in enzymatic condition when the 1000 kGy dose was applied. There was no change of weight loss of unirradiated silk fibroin in control condition over the degradation period due to the reinforcement of β -sheet microcrystalline structure. However, it could be digested by protease, which treated at the amorphous phase of the silk fibroin. The results of SEM examination on the irradiated silk fibers digested by protease found that there were erosions and clefts on the fibers, which was proportional to the irradiation dose. These showed that the fibroin fibers were easy to degrade when they were irradiated with the high intensity, due to the lost tensile strength.

FT-IR spectra of irradiated silk fibroin treated by PBS and protease in Figures 4.8 and 4.9 found that the Amide I, Amide II, and Amide III were increased with increasing irradiation dose due to the weakness of peptide bond as mentioned earlier. There were two peaks appeared in the Amide I band, 1695 and 1650 cm^{-1} . The 1650 cm^{-1} peak was gradually increased with increasing irradiation dose. This showed the transformation of β -sheet structure (1695 cm^{-1}) converted to be the random coil structure (1650 cm^{-1}). The area ratio of Amide I per Amide II of digested silk fibroin was increased with increasing irradiation dose in both control and enzymatic conditions (see Tables 4.3 and 4.4). This showed the increasing portion of crystalline and amorphous phases in silk fibroin of both conditions. The hydrolysis and enzyme digestion were occurred on the amorphous phase causing the reduction of amorphous phase in silk fibroin. Therefore, the ratio of Amide I per Amide II was increased.

The results of optical density (O.D.) measurement at 280 nm of degradation products in Table 4.5 showed that the O.D. was increased with increasing of incubation period and irradiation dose. These O.D. indicated the presence of aromatic amino acids in degradation products, which were released from digested fibroin samples. The higher aromatic amino acids released, the higher O.D. was measured. The observation of protease by spectrometer found that there were aromatic amino acids consisted in

protease due to the appearance of a peak at 280 nm (Figure 4.10). Moreover, the activity of protease was maximum within 7 days, after that it would lose its activity by denaturing, which could be observed by disappearing of the 280 nm peak after 7 days.

Gel electrophoresis results in Figure 4.11 showed there were 37 and 33 kDa proteins found only in protease condition. A significant change of the 37 kDa band among different irradiation doses was observed. The band was gradually darkened from unirradiated to 1000 kGy samples indicating more proteins found in degradation products, which was proportional to intensity of radiation causing the degradation of silk fibroin. The 37 kDa band of the same sample was gradually disappeared over incubation periods. At 21 and 28 days of incubation, the 37 kDa proteins were found only in 1000 kGy samples due to the activity of protease, which was maximum within 7 days as described before. Therefore, when the activity of enzyme was low, the capacity of digestion to the lower-dose irradiated samples was decreased as well, resulting in the non-releasing of 37 kDa in the lower-dose irradiated samples. For the 33 kDa proteins, there was no change among different irradiation doses of the same incubation times. In contrast, these bands became pale over the incubation periods. Additionally, lane 2 showed molecular weight of protease (28 kDa) used in this experiment to confirm that the detected bands in lanes 7 to 10 were not occurred from protease interference.

From the results of gel electrophoresis, the two protein bands in a low-molecular weight region on the gel would be the same protein acting as a light chain of silk fibroin, which may consist of a side chain (37 kDa) branching from a parental protein (33 kDa). The 37 kDa was susceptible to the irradiation intensity and protease digestion, which could be observed for changing. The 33 kDa would be a main protein of the light chain, which was non-sensitive to the change due to irradiation. However, it could be digested by protease over the degradation period causing the pale of the 33 kDa band. The smear bands under the 33 kDa band were small proteins releasing from the degradation of the 37 kDa protein caused by protease digestion, which could be determined at the 7 days of degradation time. The 33 kDa light chain detected in this study could be a characteristic of *Bombyx mori* var. *Nangnoi-Sisaket-1*, which was different to the 25 kDa light chain of other studies that used the white-cocoon silks

from the univoltine breed (found in Europe) and bivoltine breed (found in Japan, China, and Korea) for study.

One of the goals of this study was not only reduced the degradation period of silks, but also developed the silks as biomaterials used in many biomedical purposes including tissue scaffolding devices. Hence, a capacity of cell growth on irradiated silk fibroin was determined to investigate the effect of radiation on cell attachment and proliferation. The results of this part could be discussed as follows:

1. Fibroblast cells could attach on fibroin fibers because of the smooth surface of the fibers. Figure 4.2-A showed the smooth surface of unirradiated fibers causing the best attachment of the cells as shown in Figure 4.13-0 kGy.

2. Cell growth on a smooth surface was in a form of stacking up (see Figure 4.13-0 kGy).

3. Amounts of cell attachment decreased when the fibroin's surface become rough due to the strong irradiation (see Table 4.6).

4. Cell proliferation and spreading could be promoted by the roughness surface caused by higher irradiation intensity (see Figure 4.13-1000 kGy).

Although the cells could grow on irradiated fibroin fibers, the fibers irradiated at a higher dose (1000 kGy) became fragile when immersed in cell culture media. This showed that at 1000 kGy of irradiation the fibroin fibers were degraded easily due to aggressively denature of fibroin structure.

A potential of using the silk fibroin in the patients was determined by in vitro testing with human white blood cells in order to check the biocompatibility of the degummed silks. The results found that the blank fibroin films did not activate the white blood cells in any incubation period. On the other hand, the activation from white blood cells occurred on the fibroin film growing with fibroblasts in every incubated sample. This activation could be occurred from some chemicals secreted by fibroblasts, which could induce the white blood cells to activate them. However, this activation was not seem to be harmful causing the inflammation, because the white blood cell activation was maximum within 60 min and gradually decreased. This was a normal function of the white blood cells. In contrast, if the activation was prolong more than 60 min, this would be induced the inflammation. This part could be basically confirmation about the safety of prepared silk fibroins in biocompatibility

when utilized them in areas that would be attached to biological fluids, because there was no activation from the white blood cells to the blank fibroin films. This would be good for developing silks as biomaterials or other biomedical applications.

CHAPTER VI

CONCLUSION

The results on the biodegradation of silk fibroin through gamma radiation study allow us to conclude that:

1. The gamma radiation can reduce the biodegradation period of silk fibroin. The biodegradability of silk fibroin is proportional to the irradiation intensity.
2. The gamma radiation affects directly to the fibroin's structure change involving to a susceptible degradation, which can be observed by a weakness of peptide bonds, transformation of the fibroin's secondary structure (from β -sheet to random coil), reduction of crystallinity degree, increasing of water solubility, and increasing of cleavage on silk's morphology.
3. Irradiated silk fibroin has a potential to be promoted cell growth and proliferation, which can be developed to use as biomaterial or for tissue engineering purpose.
4. Silk fibroin is harmless to use in the patients by causing no activation from the in vitro biocompatibility test. This result shows a potential for developing silks as biomaterials or other biomedical applications in the future.
5. This study can confirm that the properties of Thai-native silks (*Bombyx mori var. Nangnoi Sisaket-1*) for biomedical utilizations. It is possible to develop Thai silks as good as other biomaterials, which is a future work.

REFERENCES

1. Altman GH, Diaz F, Jakuba C, Calabro T, Horan RL, Chen J, et al. Silk-based biomaterials. *Biomaterials* 2003;24: 401-16.
2. Sonthisombat A, Speakman PT. *Silk: Queen of fibres – the concise story* 2004: 1-28.
3. Wen CM, Ye ST, Zhou LX, Yu Y. Silk-induced asthma in children: a report of 64 cases. *Ann Allergy* 1990;65: 375-8.
4. Zaoming W, Codina R, Fernandez CE, Lockey RF. Partial characterization of the silk allergens in mulberry silk extract. *J Inv Allergy Clin Immunol* 1996;6: 237-41.
5. Novakovic GV, Altman G, Horan R, Kaplan DL. Tissue engineering of ligaments. *Annu Rev Biomed Eng* 2004;6: 131-56.
6. กรมวิชาการเกษตร กระทรวงเกษตรและสหกรณ์. 30 ปี วิชาการหม่อนไหม, เอกสารวิชาการ ลำดับที่ 1/2546, ISBN 974-436-297-9. พิมพ์ครั้งที่ 1. ชุมชุมสหกรณ์ การเกษตรแห่งประเทศไทย; 2546.
7. Horan RL, Antle K, Collette AL, Wang Y, Huang J, Moreau JE, et al. In vitro degradation of silk fibroin. *Biomaterials* 2005;26: 3385-93.
8. Rigueiro JP, Elices M, Llorca J, Viney C. Tensile properties of silkworm silk obtained by forced silking. *J Appl Polym Sci* 2001;82: 1928-35.
9. Zhang H, Magoshi J, Becker M, Chen JY, Matsunaka R. Thermal properties of *Bombyx mori* silk fibers. *J Appl Polym Sci* 2002;86: 1817-20.
10. Jarujinda S. Colourway. *Textile journal* 2005 Jan-Feb;10 (56): 34-8.
11. Crotch W. *A Silkmother Rearer's Handbook*. Lowe & Bronde Ltd., London, 1956: 8-44.

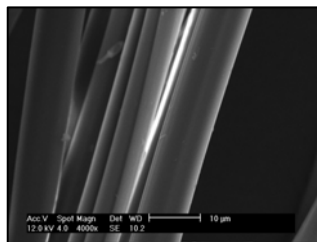
12. Altman GH, Horan RL, Lu HH, Moreau J, Martin I, Richmond JC, et al. Silk matrix for tissue engineered anterior cruciate ligament. *Biomaterials* 2003;23: 4131-41.
13. Tsubouchi K. New Applications of Silk. *Farming Japan*, 1996; 30-35: 35-41.
14. Tomihata K, Suzuki M, Oka T, Ikada Y. A new resorbable monofilament suture. *J Polym Degrad Stab* 1998;59: 13-8.
15. Inouye K, Kurokawa M, Nishikawa S, Tsukada M. Use of *Bombyx mori* silk fibroin as a substratum for cultivation of animal cells. *J Biochem Biophys Methods* 1998;37: 159-64.
16. Minoura N, Aiba S, Gotoh Y, Tsukada M, Imai Y. Attachment and growth of cultured fibroblast cells on silk protein matrices. *J Biomed Mater Res* 1995;29: 1215-21.
17. Chen G, Zhou P, Mei N, Chen X, Shao Z. Silk fibroin modified porous poly(ϵ -caprolactone) scaffold for human fibroblast culture in vitro. *J Mater Sci* 2004;15: 671-7.
18. http://en.wikipedia.org/wiki/Gamma_rays.htm
19. <http://www.epa.gov/radiation/understand/gamma.htm>
20. Thermo Nicolet Corporation. Introduction to Fourier Transform Infrared Spectrometry. 2001: 1-7.
21. <http://ww2.chem.sc.edu/chem722/WebSite/Spectroscopy/IRFrequencies.htm>
22. Gallagher W. FTIR analysis of protein structure: 1-8.
23. Sampaio S, Taddei P, Monti P, Buchert J, Freddi G. Enzymatic grafting of chitosan onto *Bombyx mori* silk fibroin: kinetic and IR vibrational studies. *J Biotec* 2005;116: 21-33.
24. Terres Jr G. Part I: Effect of hydrogen peroxide oxidation on the antigenicity of ovalbumin, bovine serum albumin, and rabbit gamma globulin. Part II: Cortical discontinuity and propagation of spreading depression [Ph.D. Thesis]. California: California Institute of Technology; 1956.
25. Shoa J, Zheng J, Lui J, Carr CM. Fourier transform Raman and Fourier transform infrared spectroscopy studies of silk fibroin. *J Appl Polym Sci* 2005;96: 1999-2004.
26. <http://www.bergen.org/AAST/projects.htm>

27. Arai T, Freddi G, Innocenti R, Tsukada M. Biodegradation of *Bombyx mori* silk fibroin fibers and films. *J Appl Polym Sci* 2004;91: 2383-90.
28. Li M, Ogiso M, Minoura N. Enzymatic degradation behavior of porous silk fibroin sheets. *Biomaterials* 2003;24: 357-65.
29. Tsuboi Y, Ikejiri T, Shiga S, Yamada K, Itaya A. Light can transform the secondary structure of silk protein. *Appl Phys A* 2001;73: 637-40.
30. Pewlong W, Sudatis B, Takeshita H, Yoshii F, Kume T. Radiation degradation of silk protein. *JAERI Conf 2000-2003*: 146-52.
31. Meesilpa P, Nuipirom W, Nakaprasert D, Sungsonthiporn S, Ravinu B, Sudatis B. Methodology to produce silk fibroin powder, unpublished 2001: 165-72.

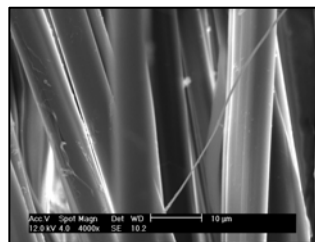
APPENDIX

Appendix A

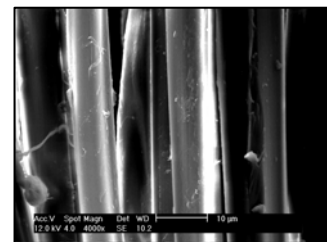
SEM images of silk fibroin irradiated at 0-1000 kGy



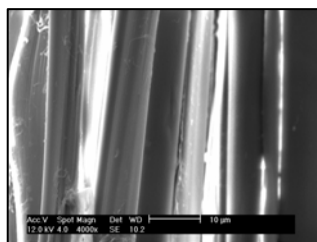
(0 kGy)



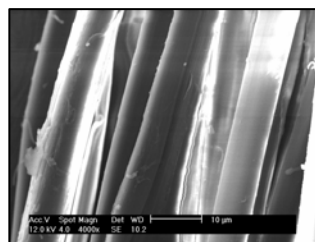
(100 kGy)



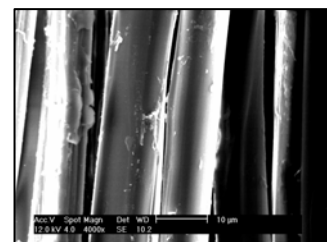
(200 kGy)



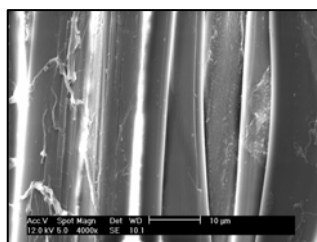
(300 kGy)



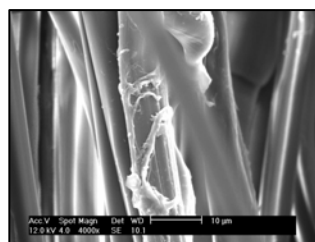
(400 kGy)



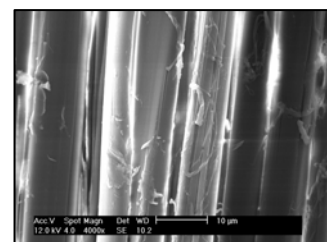
(500 kGy)



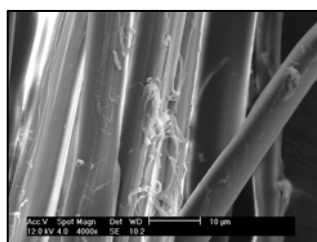
(600 kGy)



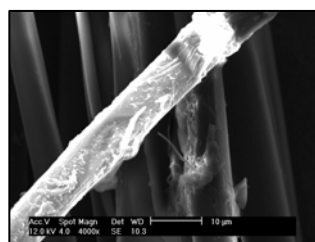
(700 kGy)



(800 kGy)



(900 kGy)



(1000 kGy)

Appendix B

A Study of Degradation Rate on Gamma Irradiated *Bombyx mori* Silk Fibroin for Biomedical Applications

Amornthep Kojthung^a, Bovornlak Oonkhanond^b

^a Department of Biomedical Engineering, Faculty of Engineering, Mahidol University

^b Department of Chemical Engineering, Faculty of Engineering, Mahidol University
25/25, Puthamonthon Sai 4 Rd., Salaya, Puthamonthon, Nakornpathom, 73170, Thailand

Abstract

Silk is the strongest natural protein fiber produced from *Bombyx mori* silkworm. Silk fibroin – a core of silk filament, has been used in medicine for centuries as a suture silk. Due to a slow degradability of silk fibroin in vivo, degrades within 2 years, it is suitable for some biomedical applications which desire long times for degrading, such as tissue scaffolding devices and suture silks. However, in some cases, residues of silk fibroin after the completed surgery can become the allergic-like proteins which can induce the host immune responses. Therefore, an attempt to reduce the degradation rate of silk fibroin through gamma radiation is then studied. The native Thai silkworm silk (*Bombyx mori* var. *Nangnoi Sisaket-1*) was chosen for studying in a form of silk film underneath an appropriate degumming time (45 min), which acquired from the FT-IR spectral analysis. Silk-fibroin films were irradiated with various doses of gamma rays (0-3000 kGy). At the higher irradiating doses from 400 to 3000 kGy, the physical properties of irradiated fibroin films were changed causing them became brittle and water dissoluble films, which indicated the degradation of silk fibroin. The time required for complete dissolution of irradiated fibroin films was decreased as applying the increasing doses. Understanding about the degradation rate of silk fibroin could be involved for developing other silk-based biomedical materials in the future.

Keywords: *Bombyx mori*; Silk fibroin; Degradation rate; Gamma radiation

1. Introduction

Silk is generally defined as a continuous protein fiber produced by some Lepidoptera larvae such as silkworms, spiders, scorpions and mites to form their cocoons [1]. The most extensively characterized silk is from *Bombyx mori* silkworms. In reality, silkworm silk is the strongest natural protein fiber, which is stronger than an equal diameter filament of steel [2]. Normally, a silk fiber consists of two types of protein, fibroin and sericin. The fibroin is a core of silk fiber, while the sericin is a glue-like protein coating on the two fibroin cores of the silk fiber. Both fibroin and sericin contains the same of 18 amino acids, but distinguishes in their amounts [2]. One of the differences between these two proteins is a crystalline structure, only the fibroin found. The crystalline structure appears in a form of $(\text{-Gly-Ala-Gly-Ala-Gly-Ser-})_n$ [3]. Due to a tremendous of crystalline structures and a high molecular weight (about 325 kDa) of polypeptide chains, these cause the fibroin being water-insoluble.

Silk is not a new biomaterial. It has been utilized in medicine as biomedical sutures for centuries. As defined by the USP, United States Pharmacopeia, silks can be categorized as non-degradable materials, because they retain greater than 50% of their tensile strength within 60 days of post-implantation in vivo [1, 4]. However, as protein polymers, silks will be proteolytically degraded and absorbed in vivo over a longer time period (within 2 years) [1]. Additionally, silks have been approved by Food and Drug Administration (FDA) for clinical uses [4, 5].

Nowadays, silks play an important role in biomedicine than the past, especially in tissue engineering. Since silk fibroin provides the great properties in biocompatibility, biodegradability, cell attachment [6], and strength, it is a suitable material to produce scaffolds used in tissue engineering tasks. A helical-wire rope scaffold is an example of silk scaffold used for anterior cruciate ligament (ACL) reconstruction produced by Altman et al [1, 7].

During the past 20 years, there have been some reports about biocompatibility problems caused by silkworm silks. However, now, there are many reports confirming that those biocompatibility problems are really caused by the contamination from the residual sericin [1, 7, 8, 9]. Therefore, to prevent an adverse effect that might be occurred to the patients, the sericin must be removed before utilizing the silks as biomedical applications. However, although the sericin is entirely removed, the biocompatibility problems may be occurred in some patients. In some cases, residues of silk fibroin after the completed surgery can become the allergic-like proteins which can induce the host immune responses [1]. From these problems, the slow degradability of silks might be one of causes. Thus, an attempt to reduce the degradation rate of silk fibroin through gamma radiation is then studied.

Gamma rays, a form of ionizing radiation, are an energetic form of electromagnetic radiation produced by radioactive decay. The gamma rays form the highest energy of electromagnetic spectrum, which can penetrate through even dense materials. According to Pewlong et al [10], the tensile strength of irradiated fibroin fiber decreased with increasing dose. The tensile strength of fibroin fiber irradiated up to 1500 kGy in oxygen decreased to 13% of non-irradiated fiber, whereas 25% for the same dose in vacuum. Furthermore, at the doses over than 2000 kGy in oxygen, the tensile strength of irradiated fiber could not be measured due to strong degradation. Therefore, it could be expected that the higher dose the fibroin irradiated, the higher solubility of the fibroin would be attained. In this study, the fibroin films were exposed to the gamma rays with various doses (0-3000 kGy) to find the optimal doses for degrading correlated with the utilization as biomedical applications.

The degradation of silk fibroin while being in the patient's body depends on several factors, but one of these factors affecting directly to the degradation is a proteolytic enzyme. Hence, to study the degradation of silk fibroin, the proteolytic enzyme should be used for digesting. According to Arai et al [11], they investigated the effects of silk fibroin on various proteolytic enzymes; collagenase Type F, α -chymotrypsin Type I-S, and protease Type XXI from *Streptomyces griseus*. They found that the protease was more aggressive than α -chymotrypsin and collagenase in silk degradation, which exhibited in the decrease of sample weight and degree of polymerization. Silks treated by protease lost their weight more than 50% within 17 days, while those treated by collagenase and α -chymotrypsin lost their weight just only 10.7% and 16.5% respectively. Furthermore, they found that the digestive capacity of the proteolytic enzymes depended on the specific peptide bonds of each enzyme. For instance, the specific peptide bond of collagenase was X – Gly bond in the sequence of X – Gly – Pro, while the α -chymotrypsin cleave the X – Y bond, where X might be an amino acid with an aromatic (Tyr, Phe, Trp) or a large hydrophobic (Val, Ile, Leu) side chain, and Y was any amino acids. In contrast, the protease was non-specificity, so it could degrade the silk fibroin more easily than the others. In this study, we did not treat the silks with any enzyme yet, it was just a preliminary study to investigate a trend of degradation of gamma irradiated silk fibroin. The degradation of silk fibroin was determined primarily by water dissolving. Whereas, changing in chemical structure of silk fibroin after gamma irradiation was analyzed by Fourier Transform Infrared Spectroscopy (FT-IR).

FT-IR spectroscopy is an analytical technique for material analysis involving an examination of the twisting, bending, rotating, and vibrational motions of atoms in a molecule. An infrared spectrum represents a fingerprint of a sample with absorption peaks which correspond to the frequencies of vibrations between the bonds of the atoms making up the material [12]. Because each different material is a unique combination of atoms, no two compounds produce the exact same infrared spectrum. Therefore, the FT-IR spectroscopy can result in a positive identification (qualitative analysis) of every different kind of material. In addition, the size of the peaks in the spectrum is a direct indication of the amount of material present. In this study, we analyzed the fibroin structure by using wavenumbers in range of 2000-600 cm^{-1} . The present of Amide I (1620 cm^{-1}), Amide II (1515 cm^{-1}) and Amide III (1230 cm^{-1}) bands showed the characteristics of silk fibroin [13]. The Amide I and Amide II bands correlated to the present of crystalline and amorphous structures in the fibroin fiber respectively [4]. The reduction of these bands indicated the degradation of the samples. Additionally, the degradation of silk fibroin can be determined by decreasing of crystallinity degree. According to Shao et al [14], the crystallinity degree of silk fibroin decreased significantly with the times of UV/ozone irradiation. Normally, the crystallinity degree of untreated silk fibroin obtained by FT-IR spectroscopy was around 48%, whereas

after treating of UV/ozone for 40 min, the crystallinity degree of irradiated silk fibroin remained about 42% which indicated the degradation of silk fibroin caused by molecular rearrangement accompanied by peptide fission [14]. The degree of crystallinity of silk fibroin could be calculated by using the two areas of Amide III (1263 and 1230). The spectral band at 1263 cm^{-1} associated with β -pleated-sheet conformation, and the band at 1230 cm^{-1} associated with random-coil conformation [14]. The crystallinity degree was calculated following by equation (1):

$$\text{Crystallinity degree (\%)} = \frac{A_{1263}}{A_{1230} + A_{1263}} \times 100 \quad (1)$$

As mentioned earlier, it was important to remove the sericin from silk fibers. Previously, there were many protocols of silk degumming to remove the sericin from silk fibers. Most protocols suggested to use the time for degumming about 60 min (including Meesilpa et al [15]), some used 30 min [16] and 10 min [17] for degumming. However, the degumming time depended on types of chemical solution used for extraction, breeds of silkworm cocoon, and a necessary to remove the sericin for final applications. In this study, we wished to remove the sericin as much as possible. Therefore, the appropriate degumming time applying to the Thai local silkworm silks (*Bombyx mori var. Nangnoi Sisaket-1*) was then studied.

The objective of this study is to be a preliminary study to investigate the degradation rate of silk fibroin through gamma radiation, which can be involved for developing and designing the resorbable silk-based biomedical materials used for various biomedical purposes in the future.

2. Materials and Methods

2.1 Cocoon degumming

Thai local silkworm cocoons (*Bombyx mori var. Nangnoi Sisaket-1*) without pupae were cut into small pieces and then degummed to remove the sericin by boiling in Na_2CO_3 solution as followed by Meesilpa et al [15]. To determine an appropriate time of degumming, the cocoons were boiled in Na_2CO_3 with different times (15, 30, 45 and 60 min). After that, the fibroin films were produced from each degummed cocoon set, and then analyzed via the FT-IR spectroscopy by compared with the FT-IR spectra of pure fibroin.

2.2 Fibroin film preparation

Degummed cocoons were dissolved in a solution containing $\text{CaCl}_2 \cdot 2\text{H}_2\text{O}$: $\text{C}_2\text{H}_5\text{OH}$: H_2O in a ratio of 1: 2: 8 by mole. Fibroin solution was then transferred into a regenerated cellulose tubular membrane (Cellusep/ T4, MWCO 12-14 kDa, Part 1430-33), and dialysis against running water for 3 days. The fibroin solution without CaCl_2 was poured on an acrylic plate, and drying at room temperature for 3 days in a laminar flow hood. After the film dried peeling the film off, the fibroin film could be stored in a desiccator for future uses.

2.3 Gamma irradiation

Fibroin films were closely packaged one package per a sample. The packaged samples were placed into a gamma irradiator (Gammacell 220 Excel, MDS Nordian). Intensity doses used in this study were 0-3000 kGy.

2.4 Dissolution of prepared silk fibroin films

Irradiated fibroin films were put into distilled water under unstirred condition at 25°C in order to observe a dissolution capability of the samples. The time required for complete dissolution to each sample was monitored.

2.5 FT-IR analysis

FT-IR spectra of each irradiated fibroin film were analyzed via a FT-IR spectrometer (Spectrum GX, PERKIN ELMER). The spectral analysis could be obtained in a range of wavenumbers 2000-600 cm^{-1} .

3. Results and discussion

3.1 Determination of appropriate degumming time

To determine an appropriate time of degumming in this work, the FT-IR spectra of samples at different degumming time (Figure 2) were compared to that of pure fibroin (Figure 1). The ratio between Amide I and Amide II areas indicated the amount of crystalline structure per amorphous structure in the sample as shown in Table 1. From the FT-IR results of degummed cocoon at various durations in Table 1, the ratio of Amide I per Amide II trended to increase from 1.3424 to be 1.6341 as increased degumming periods from 0 to 45 min, however after 45 min of degumming the Amide I per Amide II ratio was gradually decreased possibly due to the loss of crystalline phase of fibroin during degumming. Therefore, we found that the appropriate time of degumming to use with our Thai silk was 45 min which differed from other researcher's methods that usually used the white-cocoon silks for studying [4,16]. This degumming time might be a suitable condition for the yellow-cocoon Thai native silks *Bombyx mori var. Nangnoi Sisaket-1*.

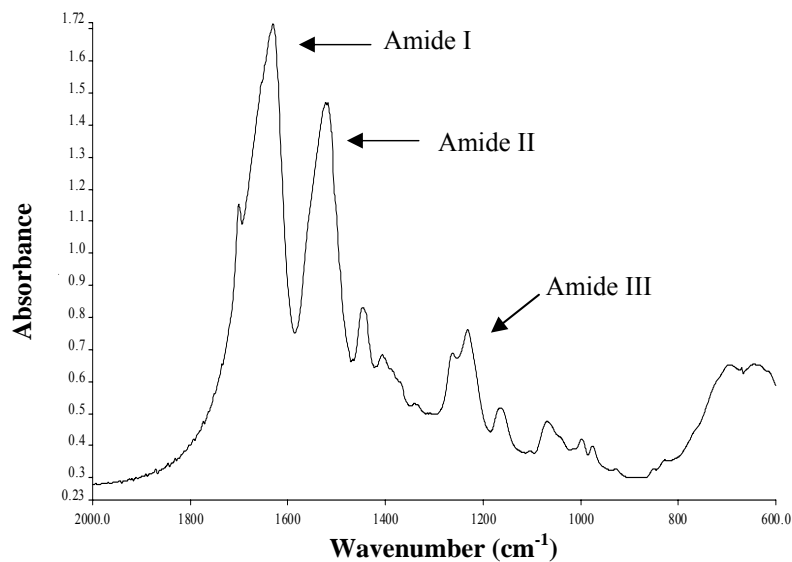


Figure 1 FT-IR spectrum of pure silk fibroin

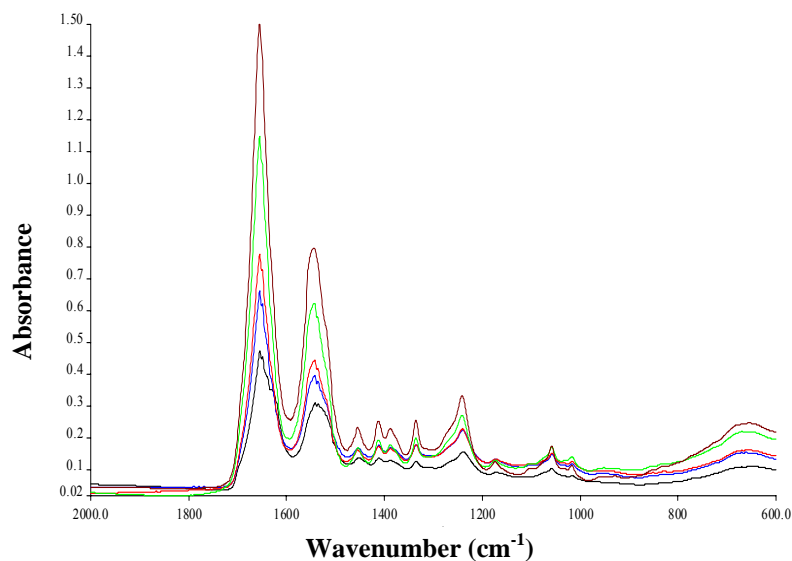


Figure 2 FT-IR spectra of fibroin in different degumming times; non-degumming (black), degumming 15 min (blue), degumming 30 min (red), degumming 45 min (green), and degumming 60 min (brown).

Table 1 Comparison of Amide I per Amide II ratio of different degumming times

Samples	Amide I (A.cm ⁻¹)	Amide II (A.cm ⁻¹)	Amide I / Amide II
Pure Fibroin	201.3946	120.0155	1.6781
Non-degumming	32.5102	24.2180	1.3424
Degumming 15 min	37.0697	27.1302	1.3664
Degumming 30 min	41.5575	28.2826	1.4694
Degumming 45 min	61.7372	37.7803	1.6341
Degumming 60 min	82.5902	52.1750	1.5829

3.2 Physical characteristic of fibroin film

Fibroin film produced from *Bombyx mori* var. *Nangnoi Srisaket-1* was pale-yellowish in color, tough, transparent and water insoluble (Figure 3). A thickness of the film was about 15 µm. A surface of the film was quite smooth with less porous structure if compared with other synthetic biomaterial films.

**Figure 3** Silk fibroin film**Table 2** Physical properties of fibroin film irradiated at various doses

Doses (kGy)	Physical properties of fibroin film
0	Pale-yellowish color, transparence, toughness and water insolubility.
100	Pale-yellowish color, transparence, toughness and water insolubility.
300	Pale-yellowish color, transparence, less toughness and water insolubility.
400	Pale-yellowish color, transparence, brittleness and water solubility.
700	Pale-yellowish color, transparence, brittleness and water solubility.
900	Pale-yellowish color, transparence, brittleness and water solubility.
1000	Brownish color, transparence, cracking, brittleness and water solubility.
2000	Brownish color, transparence, cracking, brittleness and water solubility.
3000	Brownish color, transparence, cracking, brittleness and water solubility.

All of the film samples were summarized in Table 2. The results showed that after the fibroin films were irradiated via gamma rays with doses up to 300 kGy, the films were still being like the control sample (0 kGy) in their physical appearances. While at the doses 400 – 900 kGy the films were brittle, and they became water-soluble films. Whereas at the higher range of applying doses (1000 – 3000 kGy), the color of the films was changed to be brown and they were cracked after irradiating. Furthermore, they were dissolved in water easily.

3.3 Dissolution of prepared silk fibroin films

The time required for the complete dissolution of silk fibroin samples at various irradiating doses was shown in Figure 4. The fibroin films did not dissolve in water when using the intensity less than 400 kGy, whereas over 400 kGy the fibroin films could be dissolved in water. The time required for complete dissolution was decreased linearly as the irradiating doses increased until 1000 kGy. The capacity of dissolving trended to be stable at intensity over 1000 kGy, which corresponded to the dissolution of 5 min.

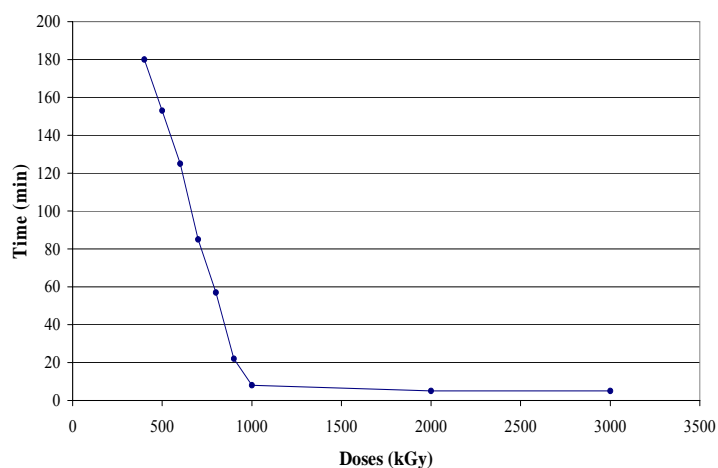


Figure 4 Water dissolution of fibroin films at various irradiating doses

4. Conclusion

From the determination of appropriate degumming time could be concluded that the appropriate time for silk degumming was 45 min, which was a suitable time condition for the Thai native silk *Bombyx mori* var. *Nangnoi Sisaket-1*.

The result of gamma irradiation to the silk fibroin films found that the gamma rays could change some physical properties of the fibroin films when applying the higher doses causing the films became brittleness and easy dissolution, which indicated the degradation of silk fibroin.

However, this study has not been completed yet. The chemical structure change due to gamma irradiation causing degradation of the silk fibroin will be studied as a future work in order to help us to understand the mechanics of degradation more clearly. Furthermore, if we can understand and control the degradation rate of silk fibroin, it would be useful for developing the silks as biomedical materials in the future.

5. Acknowledgement

We would like to thank Mr. Prateep Meesilpa, a director of The Queen Sirikit Institute of Sericulture, Thailand, who gave me the knowledge about Thai *Bombyx mori* silkworms and supported the silkworm cocoons for us.

We would like to thank Mrs. Boonya Sudatis, a chief of Radiation Entomology Section, Office of Atoms for Peace, Thailand, who gave me the knowledge about silk film preparation, and also Mr. Suriya Patcha in his kindness for doing the gamma irradiation to our samples.

References

- [1] Altman GH, Diaz F, Jakuba C, Calabro T, Horan RL, Chen J, et al. Silk-based biomaterials. *Biomaterials* 2003;24: 401-16.
- [2] Sonthisombat A, Speakman PT. Silk: Queen of fibres – the concise story 2004: 1-28.
- [3] Rigueiro JP, Elices M, Llorca J, Viney C. Tensile properties of silkworm silk obtained by forced silking. *J Appl Polym Sci* 2001;82: 1928-35.
- [4] Horan RL, Antle K, Collette AL, Wang Y, Huang J, Moreau JE, et al. In vitro degradation of silk fibroin. *Biomaterials* 2005;26: 3385-93.
- [5] Lu HH, Cooper JA, Manuel S, Freeman JW, Attawia MA, Ko FK, et al. Anterior cruciate ligament regeneration using braided biodegradable scaffolds: in vitro optimization studies. *Biomaterials* 2005;26: 4805-16.
- [6] Inouye K, Kurokawa M, Nishikawa S, Tsukada M. Use of *Bombyx mori* silk fibroin as a substratum for cultivation of animal cells. *J Biochem Biophys Methods* 1998;37: 159-64.
- [7] Altman GH, Horan RL, Lu HH, Moreau J, Martin I, Richmond JC, et al. Silk matrix for tissue engineered anterior cruciate ligament. *Biomaterials* 2003;23: 4131-41.
- [8] Wen CM, Ye ST, Zhou LX, Yu Y. Silk-induced asthma in children: a report of 64 cases. *Ann Allergy* 1990;65: 375-8.
- [9] Zaoming W, Codina R, Fernandez CE, Lockey RF. Partial characterization of the silk allergens in mulberry silk extract. *J Inv Allergy Clin Immunol* 1996;6: 237-41.
- [10] Pewlong W, Sudatis B, Takeshita H, Yoshii F, Kume T. Radiation degradation of silk protein (Private communication). *JAERI Conf 2000-2003*: 146-52.
- [11] Arai T, Freddi G, Innocenti R, Tsukada M. Biodegradation of *Bombyx mori* silk fibroin fibers and films. *J Appl Polym Sci* 2004;91: 2383-90.
- [12] Thermo Nicolet Corporation. Introduction to Fourier Transform Infrared Spectrometry. 2001: 1-7.
- [13] Sampaio S, Taddei P, Monti P, Buchert J, Freddi G. Enzymatic grafting of chitosan onto *Bombyx mori* silk fibroin: kinetic and IR vibrational studies. *J Biotec* 2005;116: 21-33.
- [14] Shao J, Zheng J, Liu J, Carr CM. Fourier transform Raman and Fourier transform infrared spectroscopy studies of silk protein. *J Appl Polym Sci* 2005;96: 1999-2004.
- [15] Meesilpa P, Nuipirom W, Nakaprasert D, Sungsonthiporn S, Ravinu B, Sudatis B. Methodology to produce silk fibroin powder (Private communication) 2001: 165-72.
- [16] Li M, Ogiso M, Minoura N. Enzymatic degradation behavior of porous silk fibroin sheets. *Biomaterials* 2003;24: 357-65.
- [17] Ha SW, Tonelli AE, Hudson SM. Structural studies of *Bombyx mori* silk fibroin during regeneration from solutions and wet fiber spinning. *Biomacromolecules* 2005;6: 1722-31.

BIOGRAPHY

NAME	Mr. Amornthep Kojthung
DATE OF BIRTH	1 April 1981
PLACE OF BIRTH	Lopburi, Thailand
INSTITUTIONS ATTENDED	Mahidol University, 2000-2004: Bachelor of Science (Medical Technology) Mahidol University, 2004-2007: Master of Engineering (Biomedical Engineering)
HOME ADDRESS	236/301, Moo 3, Saranakhom Rd., Srikan, Donmuang, Bangkok, 10210 Thailand Tel. 02-5650387 E-mail: toefiesta@yahoo.com